Chapter 10
Impact Modes and Parameter Variations

In this chapter, new parameter variation and averaging tools are introduced for impact modes. It is also shown that a specific combination of two impact modes gives another impact mode. The number of impact modes depends on the number of constraints and therefore can significantly exceed the number of degrees of freedom. The corresponding manipulations with impact modes become possible due to the availability of closed-form exact solutions obtained by means of the triangular sine temporal substitution for impulsively loaded and vibroimpact systems. In particular, the idea of van der Pol and averaging tool is adapted for the case of impact oscillator. For illustrating purposes, a model of coupled harmonic and impact oscillators is considered. Then, mass-spring systems with multiple impacting particles are considered in order to illustrate impact localization phenomena on high-energy levels.

10.1 An Introductory Example

Vibration modes with impacts have been under study for several years [23, 182, 242, 249]. In practical terms, such studies deal with the dynamics of elastic structures whose amplitudes are limited by stiff constraints. These may be designed intentionally or occur due to a deterioration of joints. As a result, such kinds of dynamics are often accompanied by a rattling noise or dither during operating regimes of vehicles or machine tools. From the theoretical standpoint, the interest to such problems is driven by the question what happens to linear normal modes as the energy of elastic vibrations becomes sufficient for reaching the constraints. Interestingly enough, some of the analytical approaches developed in the area recently found applications in molecular dynamics [68]. However, due to strong nonlinearities of the impact dynamics, most of the results relate to periodic particular solutions according to the idea of nonlinear normal modes [241]. Let us recall that the importance of linear

V. N. Pilipchuk, *Oscillators and Oscillatory Signals from Smooth to Discontinuous*,
https://doi.org/10.1007/978-3-031-37788-4_10

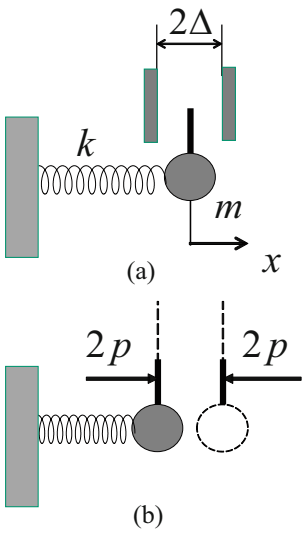

Fig. 10.1 The oscillator with bilateral rigid barriers (on the left) is replaced by the oscillator under the periodic series of external impulses (on the right)

normal modes is emphasized by the linear superposition principle as well as the parameter variation and averaging methods for weakly nonlinear cases.

Let us consider a one-degree-of-freedom free harmonic oscillator between two absolutely rigid barriers. A mechanical model of such an oscillator can be represented as a mass-spring model with two-sided amplitude limiters as shown in Fig. 10.1a.

The interaction with the barriers at $x = \pm\Delta$ is assumed to be perfectly elastic, and the system is represented in the form

$$\ddot{x} + \Omega_0^2 x = 0, \quad |x| \leq \Delta \tag{10.1}$$

Since the normal mode regimes are periodic by their definition, then the reaction of constraints can be treated as a periodic series of external impulses acting on the masses of the system.

Applying this remark to the one-degree-of-freedom system as it is shown in Fig. 10.1b, the related differential equation of motion is written in the *linear* form

$$\begin{aligned} \ddot{x} + \Omega_0^2 x &= 2p \sum_{k=-\infty}^{\infty} \left[\delta\left(\omega t + 1 - 4k + \alpha\right) - \delta\left(\omega t - 1 - 4k + \alpha\right)\right] \\ &= p\tau''\left(\omega t + \alpha\right) \end{aligned} \tag{10.2}$$

where $\delta(\xi)$ is the Dirac function, $\tau(\xi)$ is the triangular sine wave, and $2p$, ω, and α will be interpreted as arbitrary parameters.

For further convenience, the right-hand side of Eq. (10.2) is expressed through second-order generalized derivative of the triangular sine wave with respect to the

entire argument, $\omega t + \alpha$. The parameter ω will be called a frequency parameter, although it differs by the factor $\pi/2$ from the regular trigonometric frequency, $\Omega = (\pi/2)\,\omega$. Further both parameters, ω and Ω, may be used. In contrast to system (10.1), the auxiliary system (10.2) is linear but not completely equivalent to the original one as follows from the analyses below.

Representing unknown steady-state periodic solution in the form

$$x = X(\tau), \quad \tau = \tau(\omega t + \alpha) \tag{10.3}$$

gives the boundary value problem with no singular terms,

$$\omega^2 X''(\tau) + \Omega_0^2 X(\tau) = 0 \tag{10.4}$$
$$X'(\tau)\,|_{\tau=\pm 1} = p\omega^{-2}$$

and the related solution is represented in the triangle wave time form [178]

$$x = \frac{p}{\omega^2}\frac{\sin[\gamma\tau(\omega t + \alpha)]}{\gamma\cos\gamma}, \qquad \gamma = \frac{\Omega_0}{\omega} \tag{10.5}$$

This solution can be verified by direct substitution of expression (10.5) into the equation of motion (10.2).

A connection between solution (10.5) and vibration of the original system with stiff constraints is established by imposing the conditions:

- *The impulses on the right-hand side of Eq. (10.2) act when the mass strikes the limiters*

$$x = \pm\Delta \text{ if } \tau = \pm 1 \Longleftrightarrow \tau'' \neq 0 \tag{10.6}$$

- *The system cannot penetrate through the limiters; therefore,*

$$|x| \leq \Delta \text{ for all } \tau \in [-1, 1] \tag{10.7}$$

Substituting solution (10.5) into condition (10.6) determines the parameter p

$$p = \Delta\omega^2\gamma\cot\gamma \tag{10.8}$$

Substituting now (10.8) in (10.5) gives solution in the final form

$$x(t) = \Delta\frac{\sin[\gamma\tau(\omega t + \alpha)]}{\sin\gamma} \tag{10.9}$$

Obviously, solution (10.9) satisfies condition (10.6) automatically. The related parameter p (10.8) will further be treated as an eigenvalue of the nonlinear (impact)

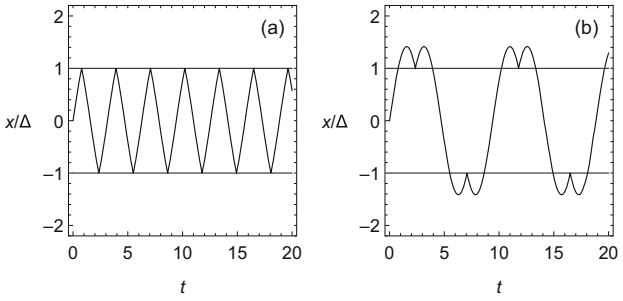

Fig. 10.2 Real (**a**) and "phantom" (**b**) solutions corresponding to the first (smallest) and second roots, respectively, $\gamma_1 = 1.1502$ and $\gamma_2 = -1.1502 + \pi$. The total energy level is $E = 1.2E_*$

problem. Other parameters, ω and α, are determined by the initial conditions. Let us assume that $x(0) = 0$ and thus $\alpha = 0$. As a result, the total energy of the oscillator per unit mass is expressed through the initial velocity as $E = [\dot{x}(0)]^2/2$. Then, taking into account (10.9) and making some analytical manipulations give

$$\gamma = \pm\frac{1}{2}\arccos\left(1 - \frac{\Omega_0^2\Delta^2}{E}\right) + k\pi, \qquad k = 0, 1, \ldots. \tag{10.10}$$

The right-hand side of expression (10.10) is a sequence of real numbers if the total energy is above its critical value, $E \geq E_* = \Omega_0^2\Delta^2/2$, such that the oscillator can reach the constraints. However, not all of the real numbers ω lead to real motions of the original system. Since the auxiliary system (10.2) has no limiters, then condition (10.6) does not guarantee that the oscillator will remain inside the region $|x| \leq \Delta$ during the period of vibration. Therefore, condition (10.7) must be verified as well. Such a verification implemented for solution (10.9) shows that condition (10.7) is satisfied only for the smallest root in set (10.10). Figure 10.2 illustrates the temporal mode shapes corresponding to the first two roots γ. It is seen that the second solution (on the right) violates condition (10.7) while satisfies condition (10.6).

Remark 10.1.1 Note that the above approach can be applied to the case of unilateral limiters. Let us remove, for instance, the left limiter and consider the oscillator (10.1) under the condition $x \leq \Delta$. In this case, the boundary conditions in (10.4) should be modified as

$$X'(\tau)\,|_{\tau=\pm1} = \pm p\omega^{-2} \tag{10.11}$$

Such a periodic change of sign effectively switches the directions of positive δ-functions on the right-hand side of Eq. (10.2). As a result, the solution takes the form

$$x(t) = \Delta \frac{\cos\left[\gamma\tau\left(\omega t + \alpha\right)\right]}{\cos\gamma} \tag{10.12}$$

where the period and the related fundamental frequency are $T = 2/\omega$ and $\Omega = \pi\omega$, respectively.

10.2 Parameter Variation and Averaging

In order to illustrate the idea of parameter variations for solution (10.9), let us include the viscous damping into the model and represent the differential equations of motion between the constraints in the form

$$\begin{aligned} \dot{x} &= v \\ \dot{v} &= -2\zeta\Omega_0 v - \Omega_0^2 x \\ |x| &\le \Delta \end{aligned} \tag{10.13}$$

where ζ is the damping ratio.

In this case, the triangle wave frequency, ω, in solution (10.9) is not constant any more, although the amplitude of the vibration remains constant as long as the oscillator is in the impact regime. The corresponding parameter variation is implemented as a change of the state variables $\{x(t), v(t)\} \to \{\gamma(t), \phi(t)\}$, dictated by solution (10.9)

$$x = \Delta \frac{\sin(\gamma\tau)}{\sin\gamma}, \qquad v = \Omega_0 \Delta \frac{\cos(\gamma\tau)}{\sin\gamma} e \tag{10.14}$$

where $\tau = \tau(\phi)$ and $e = \tau'(\phi)$ depend upon the fast phase $\phi = \phi(t)$ and $\gamma = \gamma(t)$ determines a relatively slow evolution of the temporal mode shape of the vibration.

Substituting (10.14) in (10.13) satisfies the constraint condition automatically and the system of two differential equations for new state variables

$$\begin{aligned} \dot{\gamma} &= 2\zeta\Omega_0 \cos^2\gamma\tau \tan\gamma \\ \dot{\phi} &= \frac{\Omega_0}{\gamma}[1 + \zeta(\sin 2\gamma\tau - 2\tau\cos^2\gamma\tau\tan\gamma)e] \end{aligned} \tag{10.15}$$

Below, the first-order averaging procedure is applied. Notice that the right-hand side of Eq. (10.15) is periodic with respect to the phase ϕ. As proved in Chap. 4, the averaging can be conducted with respect to the variable τ over its interval $-1 \le \tau \le 1$. As a result, one obtains

$$\dot{\gamma} = \zeta \Omega_0 \left(1 + \frac{\sin 2\gamma}{2\gamma}\right) \tan\gamma = 2\zeta\Omega_0 \left(\gamma + \frac{4}{45}\gamma^5\right) + O(\gamma^6)$$
$$\dot{\phi} = \frac{\Omega_0}{\gamma} \tag{10.16}$$

Ignoring the residual terms $O(\gamma^6)$ gives a separable equation with explicit closed-form solution for the frequency ratio

$$\gamma = \exp(2\zeta\Omega_0 t)\left[\frac{45}{4}\frac{r_0}{1 - r_0\exp(8\zeta\Omega_0 t)}\right]^{1/4} \tag{10.17}$$

The corresponding phase ϕ is obtained by using *Mathematica* package in terms of special functions

$$\phi = \Omega_0 \int_0^t \frac{dt}{\gamma} = \frac{1}{2\zeta}\left(\frac{4}{45r_0}\right)^{1/4}$$
$$\times \left\{ {}_2F_1\left[-\frac{1}{4}, -\frac{1}{4}; \frac{3}{4}; r_0\right] - \exp(-2\zeta\Omega_0 t)\right.$$
$$\left. \times [1 - r_0\exp(8\zeta\Omega_0 t)]^{5/4}\, {}_2F_1\left[1, 1; \frac{3}{4}; r_0\exp(8\zeta\Omega_0 t)\right]\right\} \tag{10.18}$$

where ${}_2F_1$ is Hypergeometric function [4] and r_0 is a constant parameter, which is calculated through the initial frequency ratio $\gamma_0 = \Omega_0/\dot{\phi}(0)$ as $r_0 = 4/(4+45\gamma_0^{-4})$.

Keeping the leading-order term only on the right-hand side of the first equation in (10.16) gives solution

$$\gamma = \gamma_0 \exp(2\zeta\Omega_0 t)$$
$$\phi = \frac{1}{2\zeta\gamma_0}[1 - \exp(-2\zeta\Omega_0 t)] \tag{10.19}$$

A simple asymptotic analysis of expressions (10.14) and the remark after expression (10.10) gives the parameter interval, $0 < \gamma < \pi/2$, within which the impact dynamics takes place. The vibration mode shapes close to the triangular wave near the left edge of the interval, but, as the energy dissipates and the parameter γ approaches $\pi/2$, vibrations become close to harmonic. The total energy is expressed through the parameter γ in the form

$$E = \frac{1}{2}\left(\frac{\Omega_0\Delta}{\sin\gamma}\right)^2 \tag{10.20}$$

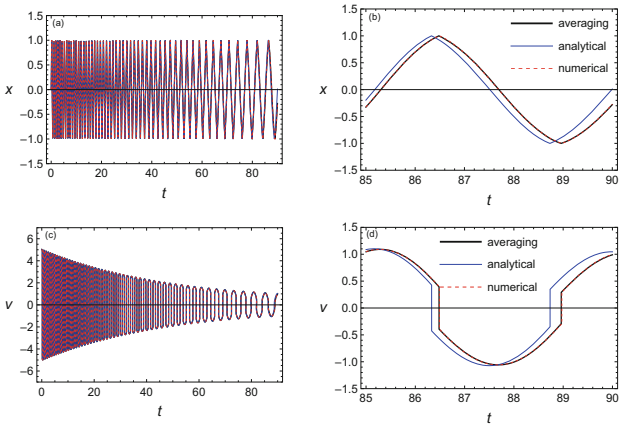

Fig. 10.3 The time history of the impact oscillator according to the numerical solution of "exact equations" (10.15), averaged Eqs. (10.16) without polynomial expansion, and the analytical closed-form solution given by (10.14), (10.17), and (10.18); the parameters are $\gamma_0 = 0.2$, $\zeta = 0.01$, $\omega_0 = 1.0$, and $\Delta = 1.0$

The duration of the impact stage of the dynamics is estimated via solution (10.19) as

$$\gamma(t_{\max}) = \frac{\pi}{2} \Longrightarrow t_{\max} = \frac{1}{2\zeta\Omega_0} \ln \frac{\pi}{2\gamma_0} \tag{10.21}$$

where $\gamma_0 = \gamma(0)$.

As follows from Fig. 10.3, the above averaging procedure leads to practically no error of the time history record within the entire interval of validity of the approach. The analytical solution based on the reduced model gives some deviation from the exact curve at the end of the impact stage of the dynamics. Notice that there is no impact interactions with the constraints for $t > t_{\max}$, where the model becomes harmonic oscillator whose amplitude exponentially decays due to the energy dissipation. At this stage, transformation (10.14) is not valid any more, nor there is any need in transformations. Still the question occurs about such solutions that would be capable of describing both impact and non-impact stages within the same closed-form expressions.

10.3 Two-Degrees-of-Freedom Model

Let us obtain first the impact mode solutions for the model shown in Fig. 10.4 under no damping condition, $c = 0$. For the sake of simplicity, let us also assume that $k_1 = k_2 = k$. On the impact normal mode motions, the system can be effectively replaced by

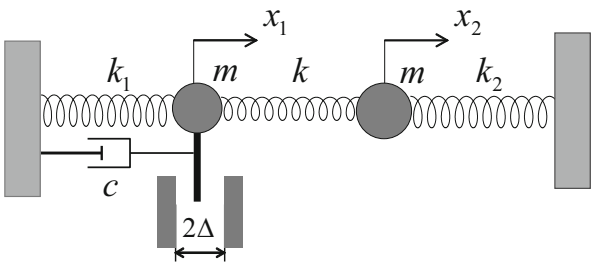

Fig. 10.4 The two-degrees-of-freedom model with viscous damping in the impact subcomponent

$$\begin{aligned} \ddot{x}_1 + \Omega_0^2 (2x_1 - x_2) &= p_1 \tau''(\omega t + \alpha) \\ \ddot{x}_2 + \Omega_0^2 (2x_2 - x_1) &= 0 \end{aligned} \tag{10.22}$$

where $\Omega_0^2 = k/m$ and the parameters ω and p_1 must provide the following condition

$$|x_1| \le \Delta \tag{10.23}$$

The impact mode solution is represented in the form

$$x_n(t) = X_n(\tau); \qquad \tau = \tau(\omega t), \qquad n = 1, 2 \tag{10.24}$$

Substituting (10.24) in (10.22) and eliminating the singular term $e'(\omega t)$ give the linear boundary value problem

$$\begin{aligned} \omega^2 X_1'' + \Omega_0^2 (2X_1 - X_2) &= 0 \\ \omega^2 X_2'' + \Omega_0^2 (2X_2 - X_1) &= 0 \end{aligned} \tag{10.25}$$

$$\begin{aligned} X_1'|_{\tau=\pm 1} &= p_1 \omega^{-2} \\ X_2'|_{\tau=\pm 1} &= 0 \end{aligned} \tag{10.26}$$

The corresponding solution has the form

$$\begin{aligned} X_1 &= \frac{p_1}{2\gamma\omega^2} \left[\frac{\sin(\gamma\tau)}{\cos\gamma} + \frac{\sqrt{3}}{3} \frac{\sin(\sqrt{3}\gamma\tau)}{\cos(\sqrt{3}\Omega_0/\omega)} \right] \\ X_2 &= \frac{p_1}{2\gamma\omega^2} \left[\frac{\sin(\gamma\tau)}{\cos\gamma} - \frac{\sqrt{3}}{3} \frac{\sin(\sqrt{3}\gamma\tau)}{\cos(\sqrt{3}\gamma)} \right] \end{aligned} \tag{10.27}$$

where $\gamma = \Omega_0/\omega$ and the "eigenvalue" p is determined by substituting X_1 into

$$X_1|_{\tau=\pm 1} = \pm\Delta \tag{10.28}$$

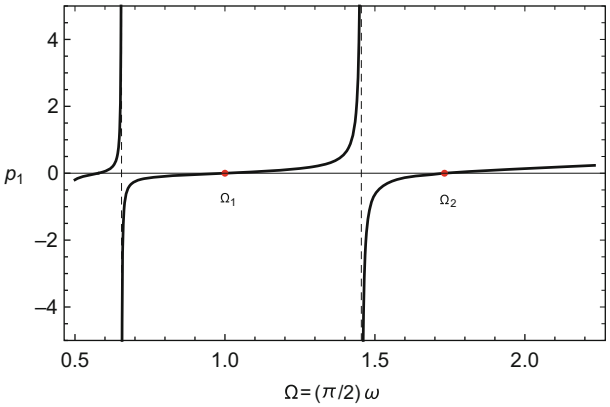

Fig. 10.5 Constraint reaction parameter p_1 versus the fundamental frequency of vibration $\Omega = (\pi/2)\,\omega$ in the case of two mass-spring model with one constrained mass; the model parameters are: $\Omega_0 = 1.0$, $\Delta = 0.2$

This gives

$$p_1 = 2\gamma\omega^2\Delta[\tan\gamma + (\sqrt{3}/3)\tan(\sqrt{3}\gamma)]^{-1} \tag{10.29}$$

In order to insure that solutions (10.27) and (10.29) describe real motions, condition (10.7) must be verified.

As follows from Fig. 10.5, the reaction impulses from amplitude limiters are positive, e.g., reflecting the mass whenever the fundamental frequency of vibrations, $\Omega = (\pi/2)\,\omega$, is on the right of any of the eigenfrequencies of the linear spectrum, $\Omega_1 = \Omega_0$ or $\Omega_2 = \sqrt{3}\Omega_0$. Note that, while on the right, Ω should still be close enough to Ω_1 in order to stay away from the next frequency, Ω_2. The situation is quite different on the right of second frequency Ω_2, corresponding to the antiphase mode. Its right neighborhood extends to the infinity with no "obstacles." It will be shown below that the condition $\Omega \gg \Omega_2$ provides the so-called mode localization. The energy outflow from such a localized mode is prevented by the impossibility of internal resonance with any of the linear modes. Recall that the damping is ignored here. In reality, the high frequency Ω cannot be maintained unless a proper energy inflow into the system is provided.

For numerical validating purposes, Fig. 10.6a, c illustrates the impact mode shapes[1] (10.27) at two different vibration frequencies Ω, such that $\Omega_1 < \Omega \ll \Omega_2$ and $\Omega_2 \ll \Omega$. In different color, the diagrams also show profiles obtained by numerical solution of a model with "soft" amplitude limiters represented by the elastic strongly nonlinear restoring force $p(t) = [x_1(t)/\alpha\Delta]^{2n-1}$, where $n = 9$ and

[1] For a better visualization purpose, here and below, displacements of mass-spring models are shown as vertical.

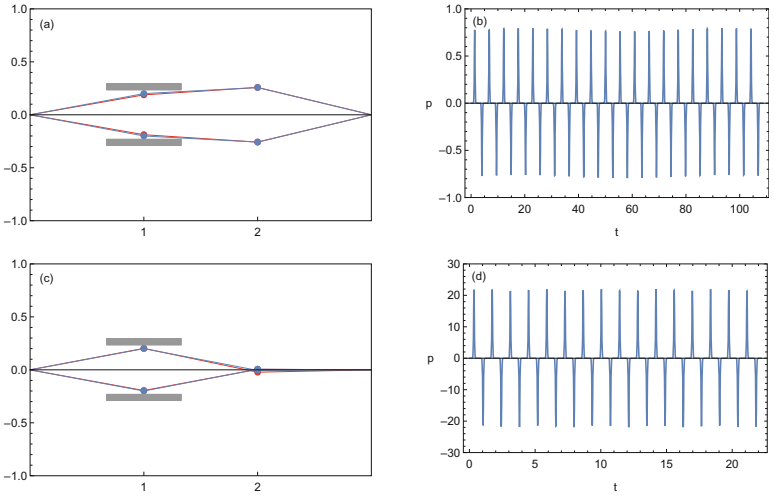

Fig. 10.6 Impact mode profiles (**a**), (**c**) and the restoring pulses (**b**), (**d**) in the right neighborhoods of the linear eigenfrequencies of the two mass-spring model with amplitude limiters imposed on the first mass; the parameters are $\Delta = 0.2$, $\Omega_0 = 1.0$, (a-b): $\omega = (2/\pi)\Omega_1 + 0.1$, and (**c**)–(**d**): $\omega = (2/\pi)\Omega_2 + 2.5$

$\alpha = 0.968$ is a numerical factor compensating the smoothing effect. An optimal number α would be obviously different for different energy levels.

10.4 A Double-Pendulum with Amplitude Limiters

The top mass m_1 of a free double-pendulum, as shown in Fig. 10.7, oscillates between the two absolutely stiff constraints providing small angular amplitudes of the top pendulum

$$\left|\varphi_1\right| \le \Delta_1 \ll 1 \tag{10.30}$$

For comparison reason, we also use a "soft version" of constraints (10.30) represented by the potential energy, which provides a fast-growing restoring force near the boundaries $\varphi_1 = \pm\Delta_1$

$$V(\varphi_1) = \frac{\beta}{2n}\left(\frac{\varphi_1}{\Delta_1}\right)^{2n}, \qquad n \gg 1 \tag{10.31}$$

where α is a positive constant parameter measured in energy units and n is an integer.

Assuming that the both rods of the double pendulum are massless and have the same length l gives the system Lagrangian

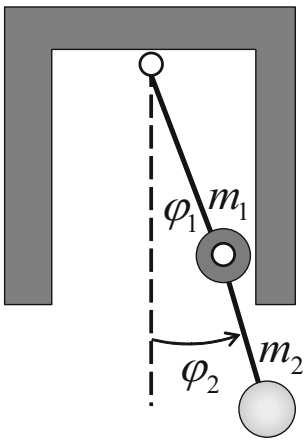

Fig. 10.7 Double pendulum with bilateral constraints

$$L = \frac{1}{2}l^2\left[(m_1+m_2)\dot{\varphi}_1^2 + 2m_2\dot{\varphi}_1\dot{\varphi}_2\cos(\varphi_1-\varphi_2) + m_2\dot{\varphi}_2^2\right]$$
$$-gl\left[m_1(1-\cos\varphi_1) + m_2(2-\cos\varphi_1-\cos\varphi_2)\right] - V(\varphi_1) \quad (10.32)$$

Due to the constraint condition, the angle φ_1 must be small. Assuming that the angle φ_2 is also small, let us approximate Lagrangian (10.32) by its quadratic form while keeping the term $V(\varphi_1)$ unchanged since the maximum ratio φ_1/Δ_1 is of order one. Using $\sqrt{g/l}t$ as a new temporal argument under the original notation t and rescaling the corresponding Euler-Lagrange equations, respectively, give

$$\mu^2\ddot{\varphi}_1 + \ddot{\varphi}_2 + \mu^2\varphi_1 = -\beta_1\left(\frac{\varphi_1}{\Delta_1}\right)^{2n-1}$$
$$\ddot{\varphi}_1 + \ddot{\varphi}_2 + \varphi_2 = 0 \quad (10.33)$$

where $\mu^2 = 1 + m_1/m_2$ and $\beta_1 = \beta/(m_2 g l \Delta_1)$ are unitless parameters and dots indicate differentiation with respect to the new temporal argument.

We seek a family of (impact mode) periodic solutions on which the reaction of constraints represents a periodic sequence of δ-functions. For that reason, we switch from system (10.32) to a linear non-autonomous system by replacing the nonlinear term as

$$-\beta_1\left(\frac{\varphi_1}{\Delta_1}\right)^{2n-1} \to p_1\tau''(\omega t+\alpha) \quad (10.34)$$

The linearized system (10.33) has normal mode vectors and natural frequencies

$$\mathbf{e}_1 = \frac{1}{\sqrt{2\mu\,(\mu+1)}}\begin{pmatrix}1\\ \mu\end{pmatrix}, \quad \Omega_1 = \sqrt{\frac{\mu}{\mu+1}}$$

$$\mathbf{e}_2 = \frac{1}{\sqrt{2\mu\,(\mu-1)}}\begin{pmatrix}1\\-\mu\end{pmatrix}, \quad \Omega_2 = \sqrt{\frac{\mu}{\mu-1}} \tag{10.35}$$

where the modal vectors satisfy the orthogonality condition, $\mathbf{e}_j^T M \mathbf{e}_i = \delta_{ji}$, with respect to the inertia matrix

$$M = \begin{pmatrix}\mu^2 & 1\\ 1 & 1\end{pmatrix}$$

Transition to the principal coordinates $\{q_1, q_2\}$ is given by

$$\begin{pmatrix}\varphi_1\\ \varphi_2\end{pmatrix} = q_1\mathbf{e}_1 + q_2\mathbf{e}_2 \tag{10.36}$$

and

$$\begin{aligned}\ddot{q}_1 + \Omega_1^2 q_1 &= \frac{p_1}{\sqrt{2\mu\,(\mu+1)}}\tau''(\omega t+\alpha)\\ \ddot{q}_2 + \Omega_2^2 q_2 &= \frac{p_1}{\sqrt{2\mu\,(\mu-1)}}\tau''(\omega t+\alpha)\end{aligned} \tag{10.37}$$

Now two-parameter families of periodic solutions for both independent oscillators (10.37) can be obtained as described in Sect. 10.1 by means of the triangle wave temporal substitution, $\tau = \tau(\omega t + \alpha)$. Substituting such solutions in (10.36) and determining the impulse parameter p_1 from the condition $\varphi_1|_{\tau=1} = \Delta_1$ bring the solution to its final form (Fig. 10.8)

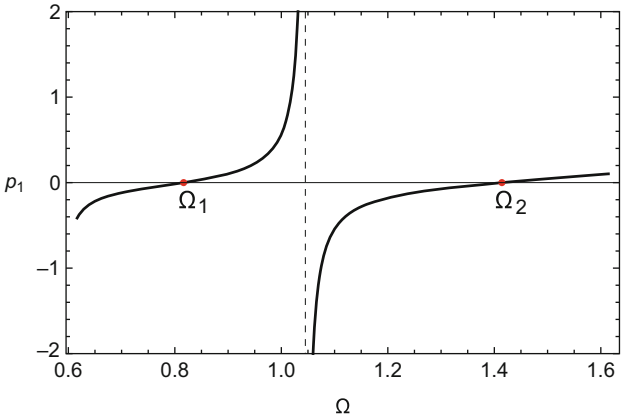

Fig. 10.8 The restoring impulse parameter versus the fundamental frequency of the double-pendulum impact mode vibration, $\Omega = (\pi/2)\,\omega$

$$p_1 = 2\gamma_1 \Delta_1 \mu(\mu+1)\omega^2 \left[\tan\gamma_1 + \left(\gamma_2/\gamma_1\right)\tan\gamma_2\right]^{-1} \tag{10.38}$$
$$= 2\Delta_1 \mu(\mu+1)\Omega_1 \omega \left[\tan\frac{\Omega_1}{\omega} + \frac{\Omega_2}{\Omega_1}\tan\frac{\Omega_2}{\omega}\right]^{-1}$$

and

$$\begin{pmatrix}\varphi_1\\ \varphi_2\end{pmatrix} = \Delta_1 \left[\tan\gamma_1 + \frac{\gamma_2}{\gamma_1}\tan\gamma_2\right]^{-1} \times \tag{10.39}$$

$$\left[\begin{pmatrix}1\\ \mu\end{pmatrix}\frac{\sin\left[\gamma_1\tau\,(\omega t+\alpha)\right]}{\cos\gamma_1} + \frac{\gamma_2}{\gamma_1}\begin{pmatrix}1\\ -\mu\end{pmatrix}\frac{\sin\left[\gamma_2\tau\,(\omega t+\alpha)\right]}{\cos\gamma_2}\right]$$

where $\gamma_{1,2} = \Omega_{1,2}/\omega$ and the relationships $\mu - 1 = \mu\Omega_2^{-2}$ and $\mu + 1 = \mu\Omega_1^{-2}$ have been used in manipulations.

Note that the frequency of first impact mode must be close enough to the first linear frequency Ω_1 to insure that it is still away from the left neighborhood of the next frequency, Ω_2. In the current case, Ω_2 is the highest frequency; therefore its right neighborhood has no upper boundary. As a result, the highest impact mode becomes spatially localized as its frequency parameter grows. The localization admits explicit estimation by the asymptotic expansion

$$\frac{\varphi_2}{\varphi_1}|_{\tau=1} = \mu\left(\tan\gamma_1 - \frac{\gamma_2}{\gamma_1}\tan\gamma_2\right)\left(\tan\gamma_1 + \frac{\gamma_2}{\gamma_1}\tan\gamma_2\right)^{-1}$$
$$= -1 - \frac{1}{3}\omega^{-2} - O\left(\omega^{-4}\right) \tag{10.40}$$

It follows from (10.40) that $(\varphi_2/\varphi_1)\,|_{\tau=1} \to -1$ as $\omega \to \infty$, so that the amplitude of the bottom mass becomes negligibly small, whereas the upper mass has the amplitude determined by the angular limiters. Figures 10.9 and 10.10 illustrate the impact mode profiles above first and second eigenfrequency of the linear spectrum, respectively. The results of numerical integration are obtained for the soft amplitude limiters represented by the high-degree potential energy (10.31) with the parameters $n = 20$ and $\beta = 0.702145$.

10.5 Averaging in the 2DOF System

Let us consider now the model shown in Fig. 10.4. The coefficient of restitution for the impact interactions is assumed to be unity, while a relatively slow energy dissipation is possible due to the viscous damping. Also, the base springs have equal stiffness, and the coupling between the oscillators is weak, such that $k_1 = k_2 =$

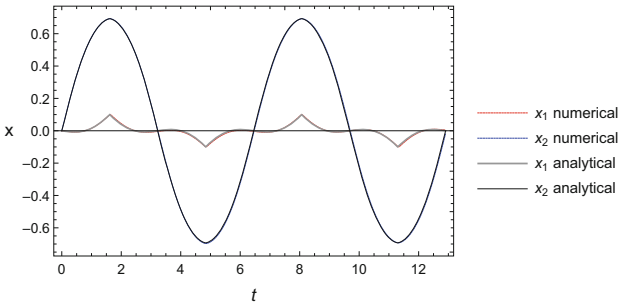

Fig. 10.9 Horizontal displacements of the top (x_1) and bottom (x_2) masses of the double-pendulum near the lower frequency of the linear spectrum, $\omega = (2/\pi)\Omega_1 + 0.1$; the system parameters are $l = 1.0$, $\Delta_1 = 0.1$, and $\mu = 2.0$

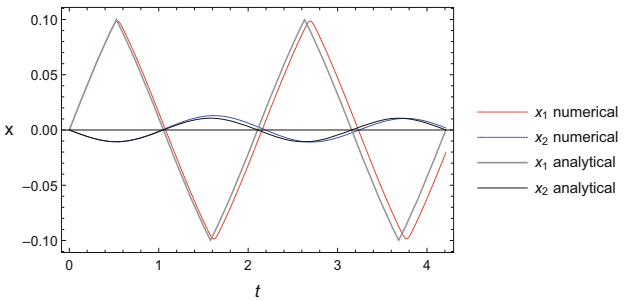

Fig. 10.10 Same as Fig. 10.9 for the frequency $\omega = (2/\pi)\Omega_2 + 1.0$; the trend to impact mode localization is developed

$K >> k$. In order to introduce the corresponding parameter variation technique, let us represent the differential equations of motion in the following general form

$$\begin{aligned}
\dot{x}_1 &= v_1 \\
\dot{v}_1 &= -f_1(x_1, x_2, v_1, v_2) + pe'(\phi) \\
\dot{x}_2 &= v_2 \\
\dot{v}_2 &= -f_2(x_1, x_2, v_1, v_2)
\end{aligned} \tag{10.41}$$

where $pe'(\phi) = p\tau''(\phi)$ and

$$\begin{aligned}
f_1(x_1, x_2, v_1, v_2) &= 2\zeta\Omega_0 v_1 + \Omega_0^2 x_1 + \beta(x_1 - x_2) \\
f_2(x_1, x_2, v_1, v_2) &= \Omega_0^2 x_2 - \beta(x_1 - x_2)
\end{aligned} \tag{10.42}$$

are impact and linear force components per unit mass, $\beta = k/m$ is the parameter of coupling, $\zeta = c/(2\Omega_0 m)$ is the damping ratio, and $\Omega_0 = \sqrt{K/m}$.

The idea of parameter variations is implemented below as a change of the state variables

$$\{x_1(t), v_1(t), x_2(t), v_2(t)\} \to \{\gamma(t), \phi(t), A(t), B(t)\}$$

according to expressions

$$\begin{aligned} x_1 &= \Delta \frac{\sin(\gamma\tau)}{\sin\gamma} \\ v_1 &= \Omega_0 \Delta \frac{\cos(\gamma\tau)}{\sin\gamma} e \\ x_2 &= A \sin\frac{\pi\tau}{2} + B\cos\frac{\pi\tau}{2} e \\ v_2 &= \Omega_0 \left(A\cos\frac{\pi\tau}{2} e - B\sin\frac{\pi\tau}{2} \right) \end{aligned} \tag{10.43}$$

where $\tau = \tau(\phi)$ and $e = e(\phi)$.

It is assumed in (10.43) that the principal frequency of the vibration, $d\phi/dt$, is dictated by the impact subcomponent rather than by a natural frequency of the corresponding linearized system. However, the scaling factor Ω_0 is still used in order to indicate the dominant oscillator of the dynamic process under consideration. Notice that $x_1$and v_1 are transformed analogously to (10.14), whereas the transformation of x_2 are v_2 is based on the standard general solution of the harmonic oscillator represented however in the nonsmooth temporal transformation form.

Substituting (10.43) in (10.41) gives

$$\begin{aligned} \dot\gamma &= \frac{e}{\Omega_0\Delta}\cos\gamma\tau \left(f_1 \sin\gamma - \Omega_0^2 \Delta \sin\gamma\tau \right) \tan\gamma \\ \dot\phi &= \frac{1}{\gamma\Omega_0\Delta}[f_1 \sin\gamma(\sin\gamma\tau - \tau\cos\gamma\tau\tan\gamma) \\ &\quad + \Omega_0^2\Delta\cos\gamma\tau(\cos\gamma\tau + \tau\sin\gamma\tau\tan\gamma)] \\ \dot A &= -\frac{1}{2}\left[\Omega_0(1-\cos\pi\tau) - \pi\dot\phi\right] B \\ &\quad + \left(\frac{1}{2}\Omega_0 A\sin\pi\tau - \frac{1}{\Omega_0} f_2 \cos\frac{\pi\tau}{2} \right) e \\ \dot B &= \frac{1}{2}\left[\Omega_0(1+\cos\pi\tau) - \pi\dot\phi\right] A + \frac{1}{\Omega_0} f_2 \sin\frac{\pi\tau}{2} - e\frac{1}{2}\Omega_0 B\sin\pi\tau \end{aligned} \tag{10.44}$$

where the functions f_1 and f_2 are expressed through the new variables by substitution (10.43) in (10.42) and the impact term $pe'(\phi)$ has been eliminated by setting (compare with (10.8))

$$p = p(t) = \Delta\Omega_0\dot{\phi}(t)\cot\gamma(t) \tag{10.45}$$

Further reduction of system (10.44) includes two major steps, such as averaging with respect to the fast phase ϕ and applying the power series expansion with respect to the parameter γ. Since the periodic functions in Eq. (10.44) are expressed through the triangular sine wave $\tau(\phi)$, then the averaging can be implemented by considering τ as an argument of the averaging as described in Chap. 4. Then, truncating the power series expansions with respect to γ gives

$$\begin{aligned}
\dot{\gamma} &= 2\zeta\Omega_0\gamma - \frac{2\beta}{\pi\Omega_0}\frac{B}{\Delta}\gamma^2 + O(\gamma^3)\\
\dot{\phi} &= \frac{\Omega_0}{\gamma} - \frac{2\beta}{45\Omega_0}\left(1 - 60\frac{12-\pi^2}{\pi^4}\frac{A}{\Delta}\right)\gamma^3 + O(\gamma^4)\\
\dot{A} &= -\left(\Omega_0 + \frac{\beta}{2\Omega_0} - \frac{\pi}{2}\dot{\phi}\right)B\\
\dot{B} &= \left(\Omega_0 + \frac{\beta}{2\Omega_0} - \frac{\pi}{2}\dot{\phi}\right)A - \frac{4\beta\Delta}{3\Omega_0}\frac{12-\pi^2}{\pi^4}\gamma^2 - \frac{4\beta\Delta}{\pi^2\Omega_0} + O(\gamma^3)
\end{aligned} \tag{10.46}$$

Approximate Eqs. (10.46) describe only one-way interaction between the oscillators so that the first two equations can be easily solved analytically; see the above one-degree-of-freedom case. Then, substituting the result into the next two equations gives a linear set of equations with variable coefficients for $A(t)$ and $B(t)$, which can also be considered analytically. Let us skip such kind of analysis but illustrate the final result in Fig. 10.11. The diagrams show the energy versus time of the second oscillator based on numerical solutions for three different sets of equations, such as exact Eqs. (10.44), the equations obtained by averaging (not described here), and the reduced set (10.46). The solutions are in quite a good match most of the time interval; however, the solution of truncated set (10.46) shows some error near the end of the interval. This happens because the parameter γ is slowly approaching its limit magnitude $\pi/2$, at which the first oscillator stops interacting with the constraints and the entire system becomes linear. Remind that Eq. (10.46) was obtained by truncating the polynomial expansions in the neighborhood of $\gamma = 0$; as a result, the accuracy of the equations is low near the point $\gamma = \pi/2$. The precision can be significantly improved by keeping few more terms of the power series with respect to γ.

10.6 Impact Modes in Multiple Degrees of Freedom Systems

Let us consider the N-degrees-of-freedom conservative system described by the coordinate vector $\mathbf{x} = (x_1, \ldots, x_N)^T \in R^N$. The corresponding mass-spring model is shown in Fig. 10.12. It is assumed that displacements of the ath mass are limited

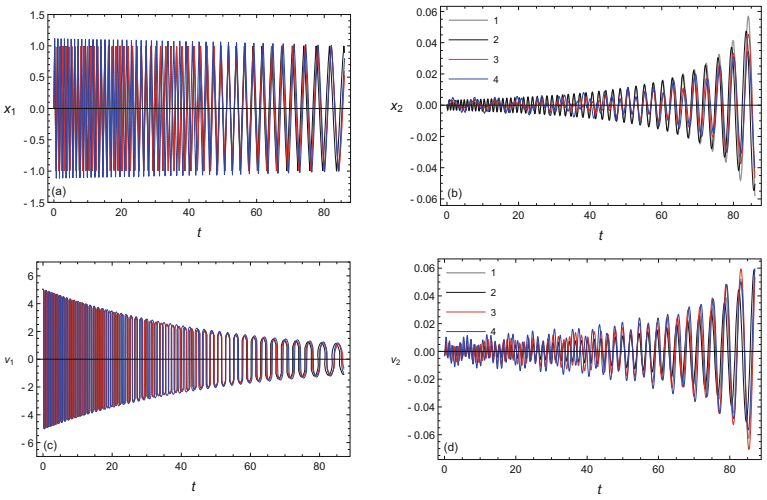

Fig. 10.11 Numerical validation of the transformed and averaged equations: (**a**)–(**b**)—mass1 and (**d**)–(**c**)—mass2. Curves: 1, averaged Eqs. (10.44); 2, the averaged equations followed by polynomial expansions (10.46); 3, Eqs. (10.44) without averaging; and 4, soft-wall approximation. The initial conditions and model parameters are as follows: $\gamma(0) = 0.2$, $\phi(0) = 0.0$, $A(0) = -0.003$, $B(0) = 0$, $\zeta = 0.01$, $\Omega_0 = 1.0$, $\Delta = 1.0$

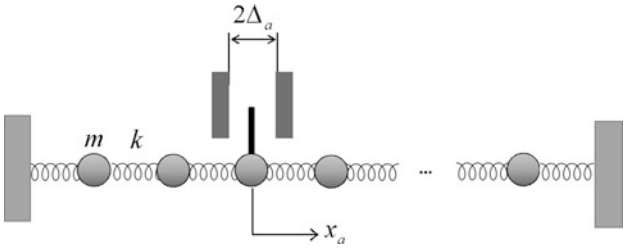

Fig. 10.12 The mass-spring model of a discrete elastic system with displacement limiters

by perfectly stiff elastic constraints, such that $|x_a| \leq \Delta_a$ or, in the matrix form,

$$\left|\mathbf{I}_a^T \mathbf{x}\right| \leq \Delta_a \tag{10.47}$$

where $\mathbf{I}_a = \left(0, \ldots, \underset{a}{1}, \ldots, 0\right)^T$.

Inside the domain (10.47), the differential equations of motion are assumed to be linear

$$M\ddot{\mathbf{x}} + K\mathbf{x} = 0 \tag{10.48}$$

where M and K are constant mass and stiffness $N \times N$ -matrixes, respectively.

The form of matrix equation (10.48) is general enough to describe different models, not necessarily mass-spring chains; see the first example below. In order to obtain impact mode solutions, the systems (10.47) and (10.48) are replaced by the following impulsively forced linear system under no constraints condition

$$M\ddot{\mathbf{x}} + K\mathbf{x} = p\mathbf{I}_a \tau''(\omega t + \alpha) \tag{10.49}$$

where p is a priori unknown "eigenvalue" and ω and α are arbitrary constant parameters.

A family of periodic solutions of the period $T = 4/\omega$ can be found as a linear superposition of solutions (10.5) for each of the N linear modes of system (10.48) with appropriate replacement of the parameters

$$\mathbf{x}(t) = \frac{p}{\omega^2} \sum_{j=1}^{N} \left(\mathbf{e}_j^T \mathbf{I}_a\right) \mathbf{e}_j \frac{\sin[\gamma_j \tau\,(\omega t + \alpha)]}{\gamma_j \cos \gamma_j}; \qquad \gamma_j = \frac{\Omega_j}{\omega} \tag{10.50}$$

where $\mathbf{e}_j$ and Ω_j are the jth normal mode and the natural frequency of linear system (10.48); it is assumed that $\Omega_i < \Omega_j$ when $i < j$, and the linear normal modes are normalized as

$$\mathbf{e}_j^T M \mathbf{e}_i = \delta_{ji} \tag{10.51}$$

where δ_{ji} is the Kronecker symbol.

The impulses act at those time instances when the ath mass interacts with the constraints; in other terms,

$$\mathbf{I}_a^T \mathbf{x} = \pm \Delta_a \text{ when } \tau = \pm 1 \tag{10.52}$$

Substituting (10.50) into (10.52), one obtains the related "eigenvalue"

$$p = \Delta_a \omega^2 \left[\sum_{j=1}^{N} (\mathbf{e}_j^T \mathbf{I}_a)^2 \frac{\tan \gamma_j}{\gamma_j} \right]^{-1} \tag{10.53}$$

where $\mathbf{e}_j^T \mathbf{I}_a$ is the ath component of the jth linear mode vector.

Substituting (10.53) into (10.50) gives a two-parameter family of the periodic solutions for the impact modes. The parameter α is an arbitrary phase shift, whereas the frequency parameter ω is subjected to some restrictions due to condition (10.47). As shown in [182], condition (10.47) is satisfied when the principal frequency of vibration, $\Omega = (\pi/2)\,\omega$, exceeds the highest frequency of the linear spectrum, $\Omega > \Omega_N$. The corresponding impact mode represents an extension of the highest linear normal mode, in which any two neighboring masses vibrate out of phase. Such an impact mode becomes spatially localized as $\Omega \to \infty$. This result was obtained also by qualitative methods in [249]. Condition (10.47) may be satisfied also when the

frequency Ω is located in a small enough right neighborhood of any frequency Ω_j and, in addition, Ω_i/Ω_j is not an odd number for all $i \neq j$. The idea of the proof is to find such cases when $\mathbf{I}_a^T\mathbf{x}$ is a monotonic function of τ on the interval $-1 \leq \tau \leq 1$, and hence condition (10.52) at the boundaries guarantees that inequality (10.47) holds inside the entire interval.

Generally, the impact modes appear to have quite a complicated spectral structure. Therefore, a detailed investigation may be required in order to formulate *necessary and sufficient* conditions of impact mode existence. However, a sufficient condition of *non-existence* can be formulated by using the physical meaning of the parameter p. Namely, if an impact mode exists, then the inequality $p(\omega) > 0$ holds. Indeed, the parameter p (10.53) cannot be negative for any real impact vibrating regime as a reaction of constraint, because it cannot be directed *toward* the barrier. Thus impact modes cannot exist when $p(\omega) < 0$.

Note that investigation of stability properties of the impact modes is rather a separate subject. Later we discuss it based on a mass-spring chain model in a semi-qualitative way.

10.7 Systems with Multiple Impacting Particles

Let us consider the case of two particles, say the ath and bth, under the constraint conditions. These conditions are $|x_a| \leq \Delta_a$ and $|x_b| \leq \Delta_b$ or, in the vector notations,

$$\left|\mathbf{I}_a^T\mathbf{x}\right| \leq \Delta_a \text{ and } \left|\mathbf{I}_b^T\mathbf{x}\right| \leq \Delta_b \tag{10.54}$$

In this case, the impulsive excitation on the right-hand side of the auxiliary equation must act on both ath and bth particles, so that the equation takes the form

$$M\ddot{\mathbf{x}} + K\mathbf{x} = (p_a\mathbf{I}_a + p_b\mathbf{I}_b)\tau''(\omega t + \alpha) \tag{10.55}$$

where p_a and p_b are parameters to be determined.

The related solution includes terms related to p_a and p_b and can be represented in the form

$$\mathbf{x}(t) = \frac{1}{\omega^2}\sum_{j=1}^{N}\left[p_a\left(\mathbf{e}_j^T\mathbf{I}_a\right)\mathbf{e}_j + p_b\left(\mathbf{e}_j^T\mathbf{I}_b\right)\mathbf{e}_j\right]\frac{\sin[\gamma_j\tau(\omega t+\alpha)]}{\gamma_j\cos\gamma_j} \tag{10.56}$$

Following the idea of normal modes, let us assume that the impact mode periodic motion is accompanied by *synchronous* impacts of both particles with the constraints according to conditions

$$\mathbf{I}_a^T\mathbf{x} = \pm\Delta_a \text{ and } \mathbf{I}_b^T\mathbf{x} = \pm\Delta_b \text{ when } \tau = \pm 1 \tag{10.57}$$

Substituting (10.56) in (10.57) gives linear algebraic equations with respect to p_a and p_b in the form

$$\begin{aligned} k_{aa}\, p_a + k_{ab}\, p_b &= \Delta_a \\ k_{ba}\, p_a + k_{bb}\, p_b &= \Delta_b \end{aligned} \tag{10.58}$$

where

$$k_{ab} = \frac{1}{\omega^2} \sum_{j=1}^{N} \left(\mathbf{e}_j^T \mathbf{I}_a\right) \left(\mathbf{e}_j^T \mathbf{I}_b\right) \frac{\tan \gamma_j}{\gamma_j} \tag{10.59}$$

Expressions (10.56) and (10.58) give a formal impact mode solution, which indeed describes an impact mode when the determinant of system (10.58) is non-zero and condition (10.54) holds. Solution (10.56) can be viewed as a strongly nonlinear superposition of the two basic impact modes with a single impacting mass.

10.7.1 Mass-Spring Chain

One Impact Particle

Let us consider a mass-spring chain of N identical particles under the constraint condition

$$m\ddot{x}_n + k\left(-x_{n-1} + 2x_n - x_{n+1}\right) = 0; \qquad n = 1, \ldots, N \tag{10.60}$$

$$x_0 = x_{N+1} = 0; \qquad |x_a| \le \Delta_a; \qquad 1 < a < N \tag{10.61}$$

where k and m are the stiffness of each spring and the mass of each particle, respectively.

The corresponding impulsively loaded linear system is represented as

$$\ddot{x}_n + \Omega_0^2\left(-x_{n-1} + 2x_n - x_{n+1}\right) = p\delta_{an}\tau''(\omega t + \alpha) \tag{10.62}$$

where $\Omega_0 = \sqrt{k/m}$ is a common physical factor for all the eigenfrequencies and the parameter of impulses p is measured per unit mass.

In this case, the corresponding linear modes and their frequencies are described exactly by expressions

$$\mathbf{e}_j = \sqrt{\frac{2}{N+1}} \left(\sin\frac{\pi j}{N+1}, \ldots, \sin\frac{N\pi j}{N+1}\right)^T \tag{10.63}$$

$$\Omega_j = 2\Omega_0 \sin \frac{\pi j}{2(N+1)}$$

where $j = 1, \ldots, N$.

Note that $j = 1+N$ formally gives the relationship[2] $\Omega_{N+1} = 2\Omega_0$, which is used below for convenience of analytical manipulations. The basis vectors of principal coordinates are normalized as $\mathbf{e}_j^T \mathbf{e}_i = \delta_{ji}$ since the inertia matrix of system (10.62) is an identity matrix. The ath component of the jth normal mode vector is therefore

$$\mathbf{e}_j^T \mathbf{I}_a = \sqrt{\frac{2}{N+1}} \sin \frac{a\pi j}{N+1} \tag{10.64}$$

where the matrix column $\mathbf{I}_a = \left(0, \ldots, \underset{a}{1}, \ldots, 0\right)^T$ was used first in (10.47).

Now adaptation of solution (10.50) and (10.53) gives in component-wise form

$$x_n = \frac{2p_a}{(N+1)\omega^2} \sum_{j=1}^{N} \sin \frac{\pi nj}{N+1} \sin \frac{\pi aj}{N+1} \frac{\sin[\gamma_j \tau\,(\omega t + \alpha)]}{\gamma_j \cos \gamma_j} \tag{10.65}$$

$(n = 1, \ldots, N)$

and

$$p_a = \Delta_a \omega^2 \left[\frac{2}{(N+1)} \sum_{j=1}^{N} \sin^2 \frac{\pi aj}{N+1} \frac{\tan \gamma_j}{\gamma_j} \right]^{-1} \tag{10.66}$$

where $\gamma_j = \Omega_j/\omega = (\pi/2)\Omega_j/\Omega$; recall that the period of triangle wave τ of is normalized to four.

For numerical illustrations below, we always set $\Omega_0 = \sqrt{k/m} = 1.0$. As follows from Eq. (10.62), the factor Ω_0 can be removed from the system by rescaling the time argument and the parameter ω. A numerical illustration of the dependence $p_a(\omega)$ and an example of the impact mode amplitude profile are given in Fig. 10.13a and b, respectively (see also Fig. 10.14). Recall that the frequency parameter ω value must provide the condition $p_a(\omega) > 0$ for the assumed restoring impulses of the amplitude limiters.

Internal Resonances

Let us discuss physical specifics in a qualitative way based on a typical temporal mode shape of an uncoupled impact oscillator

[2] Note that this is just a suitable notation since the $(N+1)$th frequency does not physically exist.

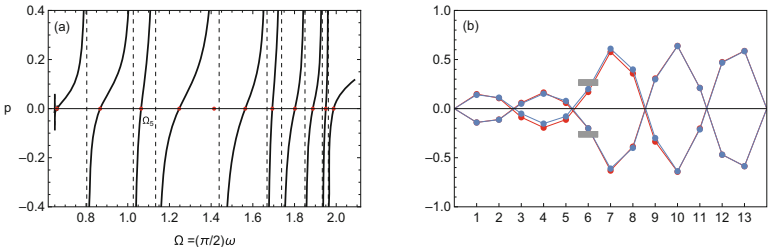

Fig. 10.13 Numerical verification of the existence of impact mode: (**a**) restoring pulses p_6 versus the fundamental frequency of vibration, Ω, for the case of one vibroimpact particle $a = 6$ ($\Delta_6 = 0.2$) of the chain of $n = 13$ particles, where the dots represent natural frequencies of the linear chain, Ω_i ($i = 3, \ldots, 13$); (**b**) the corresponding mode shape profiles for $\omega = (2/\pi)\Omega_5 + 0.02$ obtained from the analytical solution (blue) and numerical solution (red) for the soften restoring pulses represented by the force $\sim 2.18747(x_6/\Delta_6)^{17}$

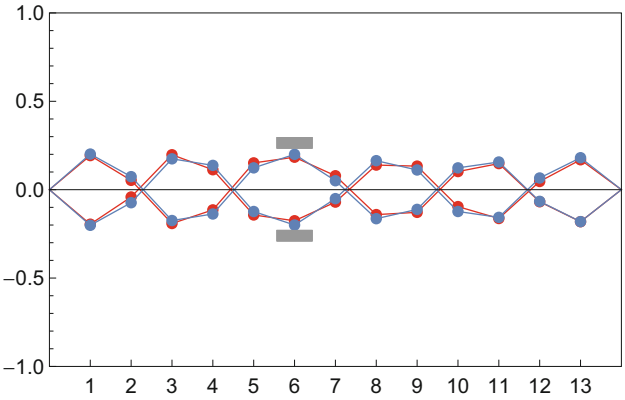

Fig. 10.14 Same as Fig. 10.13b for the case $\omega = (2/\pi)\Omega_6 + 0.02$

$$x(t) = \Delta \frac{\sin[\gamma\tau(\omega t)]}{\sin\gamma}; \qquad 0 < \gamma \le \frac{\pi}{2} \tag{10.67}$$

where γ is the parameter characterizing the energy level as shown in (10.20).

Recall that the upper boundary $\gamma = \pi/2$ corresponds to the grazing regime with the sine wave temporal shape. When $\gamma \to 0$, we have the triangle wave of an infinitely large frequency, since $\omega = O(\gamma^{-1})$ as follows from (10.5): ω and γ in (10.67) are coupled such that $\omega\gamma$ is equal to the fixed natural frequency of the oscillator without the effect of constraints. Obviously the intensive vibroimpact oscillation makes the effect of the linear part of restoring force on the time history of vibration negligible.

Let us consider the Fourier expansion of function (10.67)

$$x(t) = \Delta \sum_{s=1}^{\infty} b_s \sin[(2s-1)\Omega t], \qquad \Omega = \frac{\pi}{2}\omega \tag{10.68}$$

where Ω is the fundamental trigonometric frequency of vibration and

$$b_s = \frac{8(-1)^{s+1}\gamma \cot \gamma}{(2s-1)^2\pi^2 - 4\gamma^2} \tag{10.69}$$

The amplitude b_s is defined for any γ despite of the uncertainty at $\gamma = (2s - 1)\pi/2$, where the corresponding limit must be calculated. For illustrating purposes, let us consider the chain model described by Eq. (10.62) by imposing the temporal mode shape (10.68) on the vibroimpact particle $n = a$ as $x_a(t) = x(t)$. From the physical standpoint, such an assumption ignores the feedback from the rest of the chain to the particle $n = a$. The feedback vanishes in the asymptotic limit of intensive impacts, $\omega \to \infty$, which can be seen explicitly after switching to the phase variable ωt in Eq. (10.62). The kinematic constraint on the displacement $x_a(t)$ effectively splits the chain into two shorter chains with $N_1 = a - 1$ and $N_2 = N - a$ particles. Each of the two chains has one end fixed and another one oscillating according to dependence (10.68). Both chains obey the differential equations of the same form with either $N = N_1$ or $N = N_2$

$$\ddot{x}_n + \Omega_0^2 (-x_{n-1} + 2x_n - x_{n+1}) = \delta_{Nn}\Omega_0^2 \Delta \sum_{s=1}^{\infty} b_s \sin[(2s-1)\Omega t] \tag{10.70}$$

where δ_{Nn} is Kronecker's symbol, $n = 1, \ldots, N$, and $N = N_\alpha$ ($\alpha = 1, 2$).

System (10.70) is solved by taking into account (10.63) and switching to the principal coordinates q as

$$\mathbf{x} = \sum_{j=1}^{N} q_j(t)\mathbf{e}_j \tag{10.71}$$

gives the differential equation for the jth mode

$$\ddot{q}_j + \Omega_j^2 q_j = \Omega_0^2 \left(\mathbf{e}_j^T \mathbf{I}_N\right) \Delta \sum_{s=1}^{\infty} b_s \sin[(2s-1)\Omega t] \tag{10.72}$$

The corresponding steady-state (particular) solution is

$$q_j = \Omega_0^2 (\mathbf{e}_j^T \mathbf{I}_N) \Delta \sum_{s=1}^{\infty} \frac{b_s \sin[(2s-1)\Omega t]}{\Omega_j^2 - (2s-1)^2\Omega^2} \tag{10.73}$$

where

$$\mathbf{e}_j^T \mathbf{I}_N = \sqrt{\frac{2}{N_\alpha + 1}} \sin \frac{N_\alpha \pi j}{N_\alpha + 1}$$

$$\Omega_j = 2\Omega_0 \sin \frac{\pi j}{2(N_\alpha + 1)}; \qquad \alpha = 1, 2 \tag{10.74}$$

Taking into account (10.74) and the numbers $N_1 = a - 1$ and $N_2 = N - a$ gives

$$\Omega = \frac{\pi}{2}\omega = \frac{2\Omega_0}{2s - 1} \sin \frac{\pi j}{2a}; \qquad j = 1, \ldots, N_1 \tag{10.75}$$

$$\Omega = \frac{\pi}{2}\omega = \frac{2\Omega_0}{2s - 1} \sin \frac{\pi j}{2(N - a + 1)}; \qquad j = 1, \ldots, N_2 \tag{10.76}$$

where $1 < a < N$ and $s = 1, 2, \ldots$.

Since resonance frequencies (10.75) and (10.76) are obtained by splitting the chain in two separate pieces by inserting the vibroimpact oscillator in between two subsystems and ignoring possible feedback, then let us clarify how "exact solution" (10.65) does behave under the input frequencies estimated by (10.75) and (10.76). Note that, in contrast to solution (10.73), solution (10.65) does not have singularities at frequencies (10.75) and (10.76). Still Fig. 10.15 depicts sharp increases of the corresponding amplitudes confirmed also by the results of numerical integration under soften constraint conditions. Further, Fig. 10.16 illustrates the trend to impact mode localization as the input frequency ω exceeds the highest resonance frequency by about 6%. The fragment (a) shows a match of mode profiles obtained from different solutions and represented by different colors on the same graph. Recall that solution (10.73) is applied separately to the left and right parts of the chain by using (10.74) with $\alpha = 1$ and $\alpha = 2$, respectively. Also, modal vectors (10.63) must be calculated separately for the numbers of particles N_1 and N_2, respectively. Finally, when switching back to the coordinates $\mathbf{x}$ by means of expansion (10.71), the particles of the right part of the chain, which is after the inserted vibroimpact particle, $n = a$, must be taken in the reverse way: $n =$

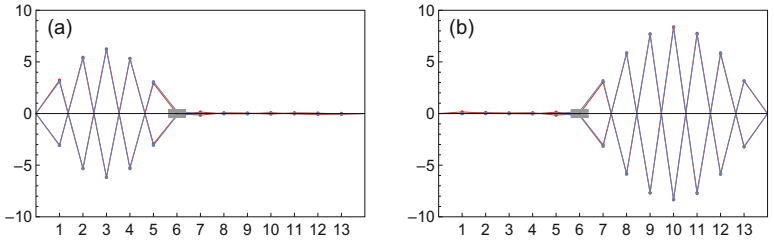

Fig. 10.15 Impact mode profiles associated with resonance frequencies: (**a**) (10.75) for $\omega = 1.22985$ ($j = N_1$) and (**b**) (10.76) for $\omega = 1.24877$ ($j = N_2$); both shapes are obtained for the chain parameters: $n = 13$, $a = 6$, $\Delta_6 = 0.2$, and $\Omega_0 = 1.0$, using analytical solution (10.65) and numerical integration with constraints replaced by the restoring force $1.73828(x_6/\Delta_6)^{17}$

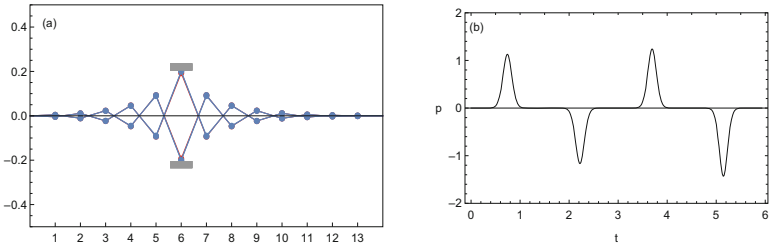

Fig. 10.16 Validation of analytical solutions for the frequency, $\omega = 1.34877$ ($j = N_2$): (**a**) impact mode profiles obtained from solutions (10.65), (10.71)–(10.73), and numerical solution for the chain with soft amplitude limiters described by the restoring force replaced by the restoring force $1.73828(x_6/\Delta_6)^{17}$, and (**b**) initial phase of the restoring pulses from the soft amplitude limiters

$N_2,\ldots,1$. The fragment (b) of Fig. 10.16 illustrates the temporal profile of restoring pulses produced by the soften amplitude limiters. Obviously such pulses are not perfectly localized, and their timing cannot perfectly match the collision times dictated by the auxiliary system (10.62) through the frequency ω. As a result, the smoothed pulses (Fig. 10.16b) may eventually desynchronize and corrupt the spatial mode profile as compared to the analytical predictions. A long-term simulation nonetheless confirms that the localization of amplitude envelope is maintained. This happens because, for the given frequency ω, the spectrum of vibroimpact oscillator has no intersections with the natural spectra of both left and right parts of the chain. As a result, no more or less significant energy exchange between the vibroimpact oscillator and the rest of the chain can occur.

Two Impact Particles

Since the auxiliary system (10.62) is linear, then adding more impulsive terms to its right-hand side will result in a linear combination of solutions similar to (10.65). For instance, if two masses, $n = a$ and $n = b$, are interacting with their amplitude limiters, then solution (10.65) is generalized as

$$x_n = \frac{2}{(N+1)\omega^2} \times \sum_{j=1}^{N} \left(p_a \sin\frac{\pi a j}{N+1} + p_b \sin\frac{\pi b j}{N+1} \right) \sin\frac{\pi n j}{N+1} \frac{\sin[\gamma_j \tau\,(\omega t + \alpha)]}{\gamma_j \cos\gamma_j} \quad (n = 1, \ldots, N) \tag{10.77}$$

Recall that the original system is strongly nonlinear due to its inherent impacts. Therefore any conventional linear modal superposition is impossible. In the present case, it follows from the fact that the parameters of restoring pulses, p_a and p_b, are

not independent but coupled by algebraic system (10.58). This system is fortunately linear and thus admits solution

$$p_a = \frac{\Delta_a k_{bb} - \Delta_b k_{ab}}{k_{aa}k_{bb} - k_{ab}k_{ba}}$$
$$p_b = \frac{\Delta_b k_{aa} - \Delta_a k_{ba}}{k_{aa}k_{bb} - k_{ab}k_{ba}} \tag{10.78}$$

where

$$k_{ab} = \frac{2}{(N+1)\omega^2}\sum_{j=1}^{N} \sin\frac{\pi aj}{N+1}\sin\frac{\pi bj}{N+1}\frac{\tan\gamma_j}{\gamma_j}, \qquad \gamma_j = \Omega_j/\omega \tag{10.79}$$

and $\{\Omega_j\}$ is the (linear) natural spectrum of the chain.

Furthermore, for the impulses to be restoring, both numbers, p_a and p_b, must be positive. This imposes certain conditions on the range of frequencies ω as seen from the illustrating example in Fig. 10.17. For instance, both restoring pulses are positive near frequency Ω_9 which is indicated by the fifth red dot from the left. Then, Fig. 10.18 illustrates the spatial mode shape profile of the corresponding impact vibration given by solution (10.77).

High-Frequency Limits and Impact Localization

Let us show that the impact mode periodic solution (10.65) becomes localized as $\omega \to \infty$ or $\gamma_j \to 0$. First, replacing the trigonometric functions by their asymptotic estimates $\sin(\gamma_j\tau) \sim \gamma_j\tau$, $\cos\gamma_j \sim 1$, and $\tan\gamma_j \sim \gamma_j$ and using the standard trigonometric sums [71] give

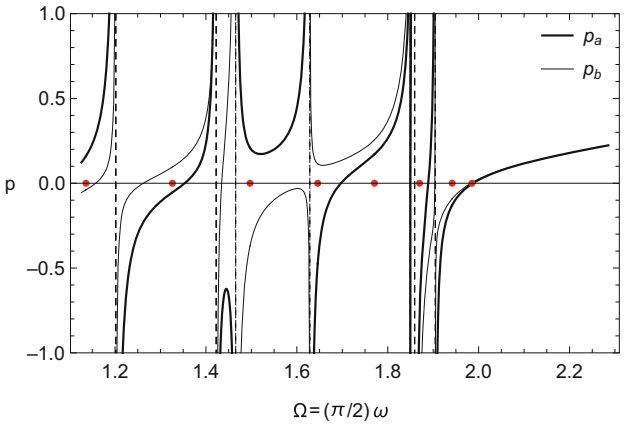

Fig. 10.17 Restoring pulses p_a and p_b versus the fundamental frequency of vibration, Ω, for the case of two vibroimpact particles $a = 5$ and $b = 9$ of the chain of $N = 12$ particles; the dots represent natural frequencies of the linear chain, Ω_i $(i = 5, \ldots, 12)$

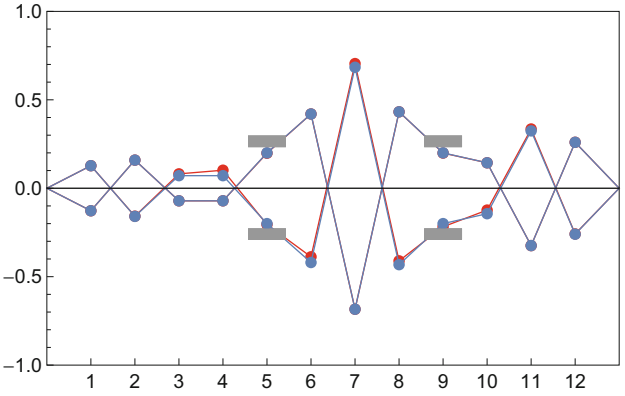

Fig. 10.18 Spatial impact mode shapes for the frequency parameter $\omega = (2/\pi)\Omega_9 + 0.02$ obtained from both analytical (black) and numerical (red) solutions after one cycle of vibration; the numerical integration is using the soften constraints represented by the restoring force $\sim (x_{a,b}/\Delta_{a,b})^{17}$

$$x_n \sim \frac{2p_a}{(N+1)\omega^2} \sum_{j=1}^{N} \sin\frac{\pi nj}{N+1} \sin\frac{\pi aj}{N+1} \tau\,(\omega t + \alpha) \qquad (10.80)$$

$$= \frac{p_a}{\omega^2} \delta_{an} \tau\,(\omega t + \alpha)$$

where δ_{an} is Kronecker's symbol, and

$$p_a \sim \Delta_a \omega^2 \left[\frac{2}{(N+1)} \sum_{j=1}^{N} \sin^2 \frac{\pi aj}{N+1} \right]^{-1} = \Delta_a \omega^2 \qquad (10.81)$$

Substituting then (10.81) in (10.80) gives

$$x_n \sim \Delta_a \delta_{an} \tau\,(\omega t + \alpha) \qquad \text{as} \qquad \omega \to \infty \qquad (10.82)$$

Expression (10.82) shows that the ath particle of the chain vibrates according to the triangle wave temporal mode shape with the infinitely large frequency, whereas all the other particles are at rest. Therefore, the impact mode becomes spatially localized as $\omega \to \infty$.

Let us consider the higher-frequency domain, $(\pi/2)\,\omega >> \Omega_N$, for the above example of mass-spring system with two impact particles, (10.77) through (10.79). In this case, $\tan(\Omega_j/\omega) > 0$ for all $j = 1, \ldots, N$, and therefore, the coefficients k_{ab} (10.79) create the so-called Gram matrix with a non-zero determinant [30], $k_{aa}k_{bb} - k_{ab}k_{ba} \neq 0$. Besides, the asymptotic estimation below confirms this

conclusion. First, the above assumption gives $\gamma_j = \Omega_j/\omega \ll \pi/2$ and the following asymptotic estimate

$$\frac{\sin(\gamma_j \tau)}{\gamma_j \cos\gamma_j} = \tau + \frac{1}{2}\gamma_j^2\left(\tau - \frac{\tau^3}{3}\right) + O\left(\gamma_j^4\right) \tag{10.83}$$

Then substituting (10.83) in (10.77) and using the trigonometric sum [71]

$$\frac{2}{(N+1)}\sum_{j=1}^{N}\sin\frac{\pi n j}{N+1}\sin\frac{\pi a j}{N+1}\gamma_j^2$$

$$= \frac{1}{4}\gamma_{N+1}^2(-\delta_{a,n-1} + 2\delta_{a,n} - \delta_{a,n+1})$$

give

$$x_n = \omega^{-2}\left(p_a\delta_{an} + p_b\delta_{bn}\right)\tau - \frac{1}{8}\omega^{-2}\gamma_{N+1}^2\left(\tau - \frac{\tau^3}{3}\right)\times \tag{10.84}$$

$$\times\left[p_a\left(\delta_{a,n-1} - 2\delta_{an} + \delta_{a,n+1}\right) + p_b\left(\delta_{b,n-1} - 2\delta_{bn} + \delta_{b,n+1}\right)\right] + O\left(\omega^{-6}\right)$$

The parameters of restoring pulses, $\{p_a, p_b\}$, are determined from (10.79), where

$$k_{ab} = \omega^{-2}\delta_{ab} - \frac{1}{12}\omega^{-2}\gamma_{N+1}^2\left(\delta_{a,b-1} - 2\delta_{ab} + \delta_{a,b+1}\right) + O\left(\omega^{-6}\right) \tag{10.85}$$

Since $\omega^{-2}\gamma_{N+1}^2 = O(\omega^{-4})$, we have $k_{ab} = \omega^{-2}\delta_{ab}$ in the leading order approximation. Therefore, $\{p_a, p_b\} = \omega^2\{\Delta_a, \Delta_b\}$as $\omega \to \infty$. In this limit, the vibration energy becomes localized on the two particles vibrating between the barriers with the triangle wave temporal shape

$$x_n \sim \left(\Delta_a\delta_{an} + \Delta_b\delta_{bn}\right)\tau\left(\omega t + \alpha\right) \quad \text{as} \quad \omega \to \infty \tag{10.86}$$

According to (10.86), the particles with numbers $n \neq a$ and $n \neq b$ are at rest. However, they oscillate with amplitudes of different orders of ω^{-2} when the parameter ω takes a large but finite value. Expansion (10.84) also shows that the temporal mode shapes of particles $n = a$ and $n = b$ are nonsmooth and getting closer to the triangle wave as the frequency ω increases. The temporal mode shapes of the nearest particles, $n = a \pm 1$ and $n = b \pm 1$, have amplitudes of order ω^{-2} and appear to be twice continuously differentiable with respect to time, t. In particular, calculating directly first two derivatives and taking into account that $\tau'^2 = 1$ give

$$\frac{d}{dt}\left(\tau-\frac{\tau^3}{3}\right)=\omega\left(1-\tau^2\right)\tau'\in C^1(R)$$

$$\frac{d^2}{dt^2}\left(\tau-\frac{\tau^3}{3}\right)=\omega^2\left[-2\tau\tau'^2+\underline{\left(1-\tau^2\right)\tau''}\right]=-2\omega^2\tau\in C(R)$$

where prime denotes differentiation with respect to the whole argument of the triangle wave, $\tau' \equiv d\tau/d(\omega t+\alpha)$; recall that the underlined terms are zero[3] because $1-\tau^2=0$ on the set of points $\{t:\tau(\omega t+\alpha)=\pm 1\}$, where $\tau''\neq 0$.

The Case of Multiple Impact Particles

A formal extension of relationships (10.56) through (10.59) on the case of multiple vibroimpact particles is quite straightforward. For instance, solution (10.56) is generalized as

$$x_n(t)=\frac{1}{\omega^2}\sum_{j=1}^{N}\sum_{i\in\sigma}p_i(\mathbf{e}_j^T\mathbf{I}_i)(\mathbf{e}_j\mathbf{I}_n)\frac{\sin[\gamma_j\tau(\omega t+\alpha)]}{\gamma_j\cos\gamma_j}=\frac{2}{(N+1)\omega^2}\times$$

$$\times\sum_{j=1}^{N}\sum_{i\in\sigma}p_i\sin\frac{\pi ij}{N+1}\sin\frac{\pi nj}{N+1}\frac{\sin[\gamma_j\tau(\omega t+\alpha)]}{\gamma_j\cos\gamma_j} \qquad (10.87)$$

$$(n=1,\ldots,N)$$

where the inner summation index covers locations of the vibroimpact particles, $\sigma\subset\{1,\ldots,N\}$.

As a result, system (10.58) takes the form

$$\sum_{i\in\sigma}k_{in}p_i=\Delta_n,\qquad n\in\sigma \qquad (10.88)$$

where

$$k_{in}=\frac{1}{\omega^2}\sum_{j=1}^{N}(\mathbf{e}_j^T\mathbf{I}_i)(\mathbf{e}_j^T\mathbf{I}_n)\frac{\tan\gamma_j}{\gamma_j} \qquad (10.89)$$

$$=\frac{2}{(N+1)\omega^2}\sum_{j=1}^{N}\sin\frac{\pi ij}{N+1}\sin\frac{\pi nj}{N+1}\frac{\tan\gamma_j}{\gamma_j}$$

are the elements of $n_\sigma\times n_\sigma$ square matrix, where n_σ is length of the list σ.

[3] It gives a zero contribution into the related integrals of the theory of distributions.

10.8 Modeling the Energy Loss at Perfectly Stiff Barriers

In this section, we follow reference [191], where the methodology of the present chapter was generalized on the case of inelastic interactions with amplitude limiters. The present modeling is based on the assumption that both the moving mass and barriers (walls) are perfectly stiff. An illustrating one degree-of-freedom model is shown in Fig. 10.1. In other words, (elastoplastic) collision deformations are assumed to be negligible as compared to rigid-body displacements, while each collision event happens momentarily. Nevertheless, even under such assumptions, terms *elastic* and *inelastic* (*plastic*) collisions are typically used in the literature in order to characterize reversible and irreversible parts of the kinetic energy, respectively. A one-dimensional collision of a moving mass with stiff obstacles is described in a phenomenological way as a discontinuity of the velocity changing its direction and magnitude as

$$\dot{x}(t_i + 0) = -k\dot{x}(t_i - 0), \qquad 0 \le k \le 1 \tag{10.90}$$

where t_i is the collision time and k is the so-called coefficient of restitution, which is further represented in the form

$$k = 1 - \varepsilon \tag{10.91}$$

According to (10.91), $\varepsilon = 0$ means an elastic collision with no energy loss, whereas $\varepsilon = 1$ is a perfectly plastic limit, when all the kinetic energy momentarily dissipates as the particle strikes an obstacle. In this section, the energy loss due to collisions is assumed to be small so that

$$0 < \varepsilon \ll 1 \tag{10.92}$$

Note that condition (10.90) fixes the time arrow of the dynamics by breaking the time symmetry $t \longrightarrow -t$ similarly to the viscous term $2\zeta\Omega\dot{x}$ of the linear oscillator $\ddot{x} + 2\zeta\Omega\dot{x} + \Omega^2 x = 0$. On first look, such temporal asymmetry creates an obstacle for describing the vibroimpact dynamics in terms of the new time argument τ, which is viewed as an *oscillating time* periodically changing its direction in a reversible way. In other words, when dealing with the time argument τ, it is difficult to specify the *before* and *after* subdomains. Nonetheless, as a first step, let us show that the representation $x = X(\tau) + Y(\tau)e$ with $\tau = \tau(\omega t)$ and $e = e(\omega t)$ can geometrically comply with condition (10.90) assuming that a system, which is described with the coordinate $x(t)$, can maintain its periodicity due to some energy inflows. Using the differentiation rules for a continuous coordinate x gives the velocity $\dot{x} = [Y'(\tau) + X'(\tau)e]\omega$. Let us assume that collisions take place whenever $\tau = \pm 1$, and, for certainty reason, consider a collision time t_i, such that $\tau(\omega t_i) = -1$. When passing through such time point t_i, the function e switches its value from $e = -1$ to $e = +1$ as seen from the diagrams for the basis functions in Fig. 1.8. Therefore, after

cancelling the common factor ω on both sides, condition (10.90) takes the form

$$\tau = -1: \quad Y' + X' = -k\left(Y' - X'\right) \tag{10.93}$$

Now, taking into account that the function e switches its value from $e = +1$ to $e = -1$ when passing through the amplitude points, at which $\tau\ (\omega t_i) = +1$, gives

$$\tau = +1: \quad Y' - X' = -k\left(Y' + X'\right) \tag{10.94}$$

Boundary conditions (10.93) and (10.94) represent an analog of the collision model (10.90) brought by the replacement of temporal argument, $t \longrightarrow \tau$. It is shown in the next section that Eqs. (10.93) and (10.94) adequately describe the vibroimpact dynamics with energy losses caused by collisions with the barriers.

10.8.1 Free Vibrations with Impact Energy Losses

Let us consider the free vibroimpact model as shown in Fig. 10.1a. The differential equation of motion with the constraint condition is represented in the form

$$\ddot{x} + \Omega^2 x = 0, \quad |x| \leq \Delta \tag{10.95}$$

where $\Omega^2 = k/m$, and it is now assumed that the impact energy loss condition (10.90) is taking place whenever $x = \pm\Delta$.

The corresponding effective model (Fig. 10.1b) is described by

$$\ddot{x} + \Omega^2 x = pe'(\varphi) \tag{10.96}$$

In the present case of free vibrations, the frequency $\omega = \dot{\varphi}(t)$ is not fixed by the external load any more. Attributed to the bead's velocity, the quantity ω determines the temporal scale of vibrating process. Generally speaking, in the present relatively simple case, when no external forces are acting, the frequency ω can be assumed to be constant in between any two interactions with the constraints in order to find an exact piecewise solution. This can be done directly with no transition to the oscillating temporal argument τ. However, our goal is to obtain a closed-form solution using the idea of separation of motions. For that reason, the function $\omega(t)$ must be interpreted as a continuously decaying quantity during the entire time range of the process. The decay rate is associated with the energy loss due to collisions with the barriers and assumed to be relatively slow by imposing the condition (10.92). Since the mass velocity is gradually decreasing, the quantity p in Eq. (10.96) characterizing the intensity of interaction with the amplitude limiters, is considered as time dependent too. Based on the above remarks, a frequency modulated solution of Eq. (10.96) can be represented as

$$x = X(\tau) + Y(\tau)e, \tau = \tau(\varphi), e = e(\varphi) \tag{10.97}$$

where $\varphi = \varphi(t)$ is a phase function to be determined.

First time derivative of (10.97) is

$$\dot{x} = [Y'(\tau) + X'(\tau)e + Y(\tau)e'(\varphi)]\omega \tag{10.98}$$

where the notation $\dot{\varphi} = \omega$ is used.

Eliminating the formal singularity of differentiation $e'(\varphi)$ by imposing the boundary condition

$$\tau = \pm 1: \quad Y = 0 \tag{10.99}$$

and then substituting (10.97) and (10.98) in (10.96) gives the relationship

$$(\omega^2 X'' + \Omega^2 X + Y'\dot{\omega}) + (\omega^2 Y'' + \Omega^2 Y + X'\dot{\omega})e + (X'\omega^2 - p)e'(\varphi) = 0$$

leading to the boundary condition

$$\tau = \pm 1: \quad X'\omega^2 = p \tag{10.100}$$

and two equations

$$\begin{aligned} \omega^2 X'' + \Omega^2 X + Y'\dot{\omega} &= 0 \\ \omega^2 Y'' + \Omega^2 Y + X'\dot{\omega} &= 0 \end{aligned} \tag{10.101}$$

Note that the boundary value problem, (10.99), (10.100), and (10.101), for X and Y has two more unknown functions, $\omega(t)$ and $p(t)$. In order to complete the formulation, the energy loss conditions, (10.93) and (10.94), must be added as

$$\tau = \pm 1: \quad Y' \mp X' = -(1-\varepsilon)\left(Y' \pm X'\right), \quad \varepsilon = 1 - k \tag{10.102}$$

The present class of solutions is such that the amplitude limiters are reached when $\tau = \pm 1$; then taking into account (10.99) gives

$$\tau = \pm 1: \quad x = X = \pm\Delta \tag{10.103}$$

Finally, the problem formulation includes two second-order differential equations (10.101) and a set of conditions (10.99), (10.100), (10.102), and (10.103) with no discontinuities. Note that condition (10.100) includes two equations determining just one unknown quantity p. However, it is sufficient to satisfy just one equation in (10.100) and one equation in (10.103) as soon as the X-component of solution is odd with respect to τ.

Further, let us assume that the energy of the oscillator is sufficient for reaching the amplitude limiters during the time interval of interest. The evolution of such a vibrating process is assumed to have the slow temporal scale $\eta = \varepsilon t$. This phase of the process will end up with the so-called grazing state of harmonic oscillations with no energy loss since model (10.95) has no explicit damping terms. During this second phase, the frequency parameter ω becomes constant, whereas the intensity of interactions with the limiters is vanishing, $p = 0$. Since the amplitude remains fixed, let us represent the temporal shape of vibrations in the form of asymptotic expansions without explicitly present slow scale η as

$$\begin{aligned} X(\tau) &= X_0(\tau) + X_1(\tau)\varepsilon + X_2(\tau)\varepsilon^2 + O\left(\varepsilon^3\right) \\ Y(\tau) &= Y_0(\tau) + Y_1(\tau)\varepsilon + Y_2(\tau)\varepsilon^2 + O\left(\varepsilon^3\right) \end{aligned} \tag{10.104}$$

where $\tau = \tau(\varphi)$ and

$$\omega = \dot{\varphi}(t) = \omega_0(\eta) + \omega_1(\eta)\varepsilon + \omega_2(\eta)\varepsilon^2 + O\left(\varepsilon^3\right) \tag{10.105}$$

$$p = p(t) = p_0(\eta) + p_1(\eta)\varepsilon + p_2(\eta)\varepsilon^2 + O\left(\varepsilon^3\right) \tag{10.106}$$

$$\eta = \varepsilon t$$

Expansions (10.104), (10.105), and (10.106) produce the leading order boundary value problem given by equations

$$X_0'' + \lambda^2 X_0 = 0, \quad Y_0'' + \lambda^2 Y_0 = 0 \tag{10.107}$$

under the boundary conditions

$$\tau = \pm 1: \quad X_0 = \pm\Delta, \quad X_0'\omega_0^2 = p_0, \quad Y_0 = 0, \quad Y_0' = 0 \tag{10.108}$$

Solution of this linear boundary value problem can be represented in the form

$$X_0 = \Delta\frac{\sin\lambda\tau}{\sin\lambda}, \quad Y_0 \equiv 0, \quad p_0 = \frac{\Omega^2\Delta}{\lambda\tan\lambda} \tag{10.109}$$

where the time-dependent "frequency ratio" $\lambda = \lambda(\eta)$ is introduced as

$$\lambda = \frac{\Omega}{\omega_0} \tag{10.110}$$

with yet unknown function $\omega_0 = \omega_0(\eta)$.

Recall that the period of triangle wave is normalized to $T = 4$. Therefore, the "real" frequency ratio is $(2/\pi)\lambda$ with the numerical factor $2/\pi$, which is somewhat inconvenient to carry through manipulations. The physical meaning of quantity λ

will be discussed later. Further, once the function $\lambda = \lambda(\eta)$ is determined, the dependence $\omega_0 = \omega_0(\eta)$ becomes known from (10.110). Now taking into account solution (10.109) leads to the differential equations of the first-order approximation in the form

$$X_1'' + \lambda^2 X_1 = 2\omega_1 \lambda^3 \frac{\Delta}{\Omega} \frac{\sin \lambda\tau}{\sin \lambda}$$
$$Y_1'' + \lambda^2 Y_1 = -\lambda \frac{d\lambda}{d\eta} \frac{\Delta}{\Omega} \frac{\cos \lambda\tau}{\sin \lambda} \tag{10.111}$$

under the boundary conditions at $\tau = \pm 1$:

$$Y_1 = 0$$
$$Y_1' = \pm\frac{1}{2} X_0' + \left(\frac{1}{2} - \lambda \frac{\omega_1}{\Omega}\right) Y_0' = \pm\frac{1}{2}\lambda\Delta \cot \lambda \tag{10.112}$$
$$X_1 = 0$$
$$X_1' = \left(\frac{\lambda}{\Omega}\right)^2 - 2\lambda \frac{\omega_1}{\Omega} X_0' = p_1 \left(\frac{\lambda}{\Omega}\right)^2 - 2\omega_1 \lambda^2 \frac{\Delta}{\Omega} \cot \lambda$$

where $\omega_1(\eta)$, $\lambda(\eta)$, and $p_1(\eta)$ are yet unknown functions.

Solution of the boundary value problem (10.111) and (10.112) is

$$X_1 = 0, \quad Y_1 = -\frac{\Delta}{2\Omega} \frac{d\lambda}{d\eta} \left(\frac{\cos \lambda\tau}{\cos \lambda} - \tau \frac{\sin \lambda\tau}{\sin \lambda}\right) \tag{10.113}$$

provided that $\omega_1(\eta) \equiv 0$ and $p_1(\eta) \equiv 0$.

Substituting Y_1 in the second equation of the set (10.112) leads to the following first-order differential equation

$$\frac{d\lambda}{d\eta} = \frac{\Omega}{2}(1 + \cos 2\lambda) \left(1 + \frac{\sin 2\lambda}{2\lambda}\right)^{-1} \tag{10.114}$$

Assuming that $\lambda(\eta)$ is determined from (10.114) and taking into account (10.110) give the fast phase

$$\varphi = \Omega \int_0^t \frac{dt}{\lambda(\varepsilon t)} \tag{10.115}$$

Substituting zero- and first-order solutions, (10.109) and (10.113), in (10.104) and then (10.97) and (10.98) gives solution in the first asymptotic order as

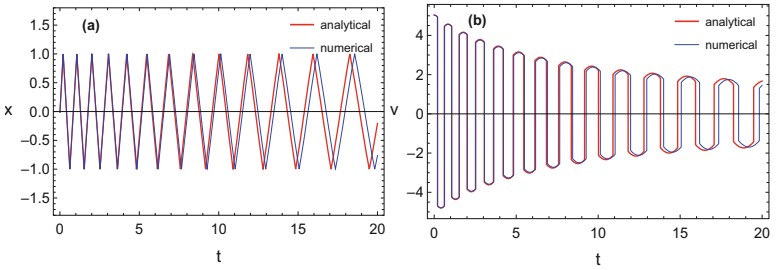

Fig. 10.19 The result of direct numerical integration and analytical approximation in first asymptotic order of ε under parameters: $\Omega = 1.0$, $\Delta = 1.0$, $\varepsilon = 0.05$, and $\omega_0(0) = 5.0$

$$x(t) = \Delta\left[\frac{\sin\lambda\tau}{\sin\lambda} - \frac{\varepsilon}{2\Omega}\frac{d\lambda}{d\eta}\left(\frac{\cos\lambda\tau}{\cos\lambda} - \tau\frac{\sin\lambda\tau}{\sin\lambda}\right)e\right] \tag{10.116}$$

$$v(t) = \Omega\Delta\left\{e\frac{\cos\lambda\tau}{\sin\lambda} + \frac{\varepsilon}{2\Omega}\frac{d\lambda}{d\eta}\left[\tau\frac{\cos\lambda\tau}{\sin\lambda} + \left(\frac{\sin\lambda\tau}{\lambda\sin\lambda} + \frac{\sin\lambda\tau}{\cos\lambda}\right)\right]\right\}$$

where $\tau = \tau(\varphi)$ and $e = e(\varphi)$ are the triangle and square waves, respectively.

Although the differential equation (10.114) is separable, the corresponding quadrature is hardly possible to find within the class of elementary functions. However, it is still well suited for a numerical solution due to the slow temporal scale $\eta = \varepsilon t$.

Solution (10.116) is illustrated in Fig. 10.19 in comparison with the result of direct numerical integration using the *Mathematica*$^{(R)}$ solver:

$$\text{NDSolve}\left[\begin{array}{c}\left\{\begin{array}{l}x''(t) + \Omega^2 x(t) = 0, x(0) = x_0, x'(0) = v_0,\\ \text{WhenEvent}\left[x(t) = \Delta, x'(t) \to -kx'(t)\right],\\ \text{WhenEvent}\left[x(t) = -\Delta, x'(t) \to -kx'(t)\right]\end{array}\right\}, \{x, t\}, \{t, 0, 15\},\\ \text{MaxSteps} \to \infty, \text{PrecisionGoal} \to 20\end{array}\right]$$

The initial conditions were calculated from (10.116) at $t = 0$. The analytical solution appeared to be in sufficient match with the numerical solution. There is some gradually developing phase shift, which is a typical effect of asymptotic approximations of frequencies in nonlinear vibrations. Let us recall that the temporal dependence for phase φ is derived from the boundary conditions, which is an essentially different way as compared to the perturbation methods in nonlinear vibrations of smooth systems [104, 151]. For that reason, note the presence of the so-called secular term with respect to τ in solution (10.116), which is still periodic with respect to the phase φ. As seen in Fig. 10.20, the intensity of strikes against the amplitude limiters, characterized by the quantity p, is diminishing with time, whereas the period of oscillations T_{imp} approaches the natural period of

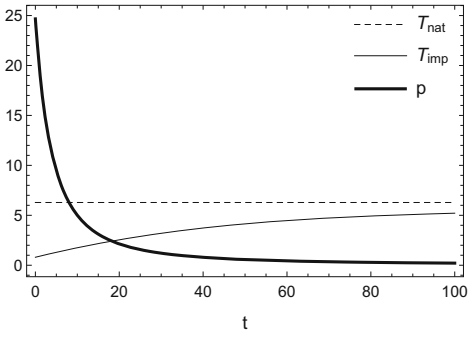

Fig. 10.20 The natural period of oscillator without impacts $T_{nat} = 2\pi/\Omega$, the period of vibroimpact cycle $T_{imp} = 4/\omega$, and the parameter of intensity of strikes against the amplitude limiters, p

unconstrained oscillator, T_{nat}. As already mentioned above, the reason is that no energy loss is assumed in between the limiters, and the system should eventually reach some "grazing" regime with near-zero impact pulses but still the same amplitude [43]. Let us support the above remarks by considering two different asymptotic cases, corresponding to high and low energy limits.

Case 1 Consider the limit $\lambda = \Omega/\omega_0 \to 0$ corresponding to either a very high initial kinetic energy or a very weak spring of the oscillator. In this case, Eq. (10.114) takes the form $d\lambda/d\eta = \Omega/2$ and gives the solution $\lambda = \Omega\eta/2 + \lambda(0)$ leading to

$$\omega_0 = \omega_0(0)\left[1 + \frac{1}{2}\omega_0(0)\eta\right]^{-1}, \quad \eta = \varepsilon t \tag{10.117}$$

and, finally,

$$\varphi = \frac{2}{\varepsilon}\ln\left[1 + \frac{1}{2}\omega_0(0)\varepsilon t\right] \tag{10.118}$$

Then solution (10.116) of the first asymptotic order is reduced to

$$x(t) = \Delta\left[\tau - \frac{1}{4}\varepsilon\left(1 - \tau^2\right)e\right], \quad \tau = \tau(\varphi), \quad e = e(\varphi) \tag{10.119}$$

where the role of "imaginary" term of order ε is to compensate deviations from straight lines between reflections against the barriers. Such deviations are due to the *continuous* representation for the phase $\varphi(t)$.

Solution (10.119) is close to the triangle wave of the gradually increasing period

$$T = \frac{4}{\omega_0(0)}\left[1 + \frac{1}{2}\omega_0(0)\varepsilon t\right] \tag{10.120}$$

Note that, according to relationship (10.117), the frequency should eventually drop to zero. This cannot happen, however, because the frequency has its lower

boundary, which is the natural frequency of harmonic oscillator itself with no interaction with amplitude limiters. For that reason, let us consider the dynamics near its low energy limit.

Case 2 The "grazing" dynamics is reached when the frequency of vibration becomes equal to the natural frequency of the oscillator, $\lambda = \Omega/\omega_0 \to \pi/2$, while the amplitude is still equal to Δ. In this case, solution (10.116) describes the harmonic temporal shape with respect the phase φ:

$$x(t) \to \Delta \sin\left[\frac{\pi}{2}\tau(\varphi)\right] \equiv \Delta \sin\left(\frac{\pi}{2}\varphi\right) \quad \text{as} \quad \lambda \to \pi/2 \tag{10.121}$$

Therefore, in this limit, the term of order ε disappears from solution (10.116) due to Eq. (10.114). Now, introducing the detuning $\rho = \pi/2 - \lambda$ and considering a small neighborhood of $\lambda = \pi/2$ bring Eq. (10.114) to the form

$$\frac{d\rho}{d\eta} = -\Omega\rho^2 + O(\rho^3) \tag{10.122}$$

with general solution $\rho = (\Omega\eta + C)^{-1}$, where C is an arbitrary constant, which is expressed through $\omega_0(0)$ by means of the equation $\lambda = \Omega/\omega_0 = \pi/2 - (\Omega\varepsilon t + C)^{-1}$. Then substituting $\lambda(\varepsilon t)$ in (10.115) and conducting integration give the phase of asymptotic solution (10.121) as

$$\frac{\pi}{2}\varphi = \Omega t + \frac{2}{\varepsilon\pi}\ln\left\{1 + \frac{\pi^2}{4}\varepsilon t\left[\omega_0(0) - \frac{2}{\pi}\Omega\right]\right\} \tag{10.123}$$

Solution (10.123) obviously holds under the condition $\omega_0(0) > (2/\pi)\Omega$, which means that initially the system must be within the impact domain. In this case, the leading term of phase is estimated by $(\pi/2)\varphi \sim \Omega t$ as $t \to \infty$, and therefore $x \sim \Delta \sin \Omega t$.

10.8.2 Bouncing Ball

Let $z = z(t)$ be the vertical upward directed coordinate of a perfectly stiff small bead, which is falling down from its initial position $z(0) = H > 0$ with zero initial velocity (Fig. 10.21). At $z = 0$, the bead reflects against the perfectly stiff floor with the coefficient of restitution $k = 1 - \varepsilon$, where $0 < \varepsilon \ll 1$. Then the bead continues to bounce until all of its energy is lost. The differential equation of motion between reflections and collision conditions is, respectively,

$$\ddot{z} = -g, \quad z \geq 0 \tag{10.124}$$

Fig. 10.21 Bouncing ball

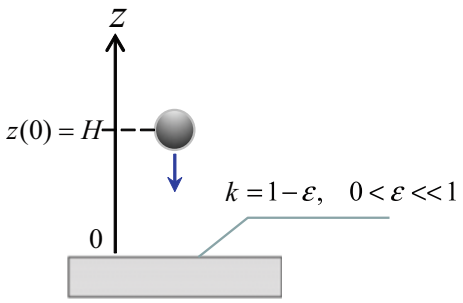

and

$$z = 0: \quad \dot{z}(t_i + 0) = -(1 - \varepsilon)\dot{z}(t_i - 0) \tag{10.125}$$

where g is acceleration due to gravity.

A presence of the linear viscosity in Eq. (10.124) would technically complicate the process of asymptotic integration although with no major effect on the analytical procedure, which is described below.

This problem has an exact piecewise parabolic solution, which is used at the end of this section for comparison reason. We use this exactly solvable problem for illustration of NSTT formalism leading to an asymptotic closed-form solution. Although the present model seems to be easier than (10.95)–(10.90), the asymptotic expansions must be generalized due to both amplitude and frequency modulation effects. The "equivalent" model, in which the reaction of constraint is represented by external pulses, takes the form

$$\ddot{z} = -g - p\,\mathrm{sgn}(\tau)e' \tag{10.126}$$

where $\tau = \tau(\varphi)$, $e' = de(\varphi)/d\varphi$, and the factor $\mathrm{sgn}(\tau)$ is to maintain the upward direction of the impulsive reaction from the stiff ground at $z = 0$.

In order to describe the combined amplitude-frequency modulation, representation (10.97) is generalized by showing the slow temporal scale, $\eta = \varepsilon t$, explicitly as

$$z = X(\tau, \eta) + Y(\tau, \eta)e \tag{10.127}$$

Further manipulations resemble the formalism of two variable expansions with an essential difference though. In particular, the differential equations of evolutionary component emerge from the boundary conditions whose role is in cancellation of δ-functions rather than eliminating resonance terms. Differentiating function (10.127) with respect to time t gives

$$\dot{z} = \frac{\partial Y}{\partial \tau}\omega + \varepsilon\frac{\partial X}{\partial \eta} + \left(\frac{\partial X}{\partial \tau}\omega + \varepsilon\frac{\partial Y}{\partial \eta}\right)e \tag{10.128}$$

$$\tau = \pm 1: \quad Y = 0 \tag{10.129}$$

Now substituting (10.128) in (10.126) and equating separately continuous, stepwise discontinuous, and impulsive groups of terms to zero in a similar to the previous section way give

$$\begin{aligned}
\frac{\partial^2 X}{\partial \tau^2}\omega^2 + \frac{\partial Y}{\partial \tau}\dot{\omega} &= -2\varepsilon\frac{\partial^2 Y}{\partial \tau \partial \eta}\omega - \varepsilon^2\frac{\partial^2 X}{\partial \eta^2} - g \\
\frac{\partial^2 Y}{\partial \tau^2}\omega^2 + \frac{\partial X}{\partial \tau}\dot{\omega} &= -2\varepsilon\frac{\partial^2 X}{\partial \tau \partial \eta}\omega - \varepsilon^2\frac{\partial^2 Y}{\partial \eta^2}
\end{aligned} \tag{10.130}$$

$$\tau = \pm 1: \quad \frac{\partial X}{\partial \tau}\omega^2 = \mp p$$

where $\omega = \dot{\varphi}$, condition (10.129) has been taken into account, and solvability of the third equation for p can be provided by imposing oddness on the derivative $\partial X/\partial \tau$ with respect to the argument τ as

$$\frac{\partial X}{\partial \tau}|_{\tau=1} = -\frac{\partial X}{\partial \tau}|_{\tau=-1} \tag{10.131}$$

It is natural to assume that the ball strikes the ground $z = 0$ whenever $\tau = \pm 1$. Then taking into account condition (10.129) gives

$$\tau = \pm 1: \quad z = X + Ye = X = 0 \tag{10.132}$$

Finally, using velocity (10.128) in (10.125) and following justifications of relationships (10.93) and (10.94) give

$$\begin{aligned}
\tau = \pm 1: \quad & \omega\left(\frac{\partial Y}{\partial \tau} \mp \frac{\partial X}{\partial \tau}\right) + \varepsilon\frac{\partial X}{\partial \eta} \\
&= -(1-\varepsilon)\left[\omega\left(\frac{\partial Y}{\partial \tau} \pm \frac{\partial X}{\partial \tau}\right) + \varepsilon\frac{\partial X}{\partial \eta}\right]
\end{aligned} \tag{10.133}$$

where the term $\partial Y/\partial \eta$ has been excluded due to condition (10.129).

Let us seek solution of the boundary value problem (10.130), (10.129), (10.133), and (10.132) in the form of asymptotic series

$$\begin{aligned}
X(\tau, \eta) &= X_0(\tau, \eta) + X_1(\tau, \eta)\varepsilon + X_2(\tau, \eta)\varepsilon^2 + O\left(\varepsilon^3\right) \\
Y(\tau, \eta) &= Y_0(\tau, \eta) + Y_1(\tau, \eta)\varepsilon + Y_2(\tau, \eta)\varepsilon^2 + O\left(\varepsilon^3\right) \\
\omega &= \dot{\varphi}(t) = \omega_0(\eta) + \omega_1(\eta)\varepsilon + \omega_2(\eta)\varepsilon^2 + O\left(\varepsilon^3\right)
\end{aligned} \tag{10.134}$$

In the leading order approximation, the boundary value problem

$$\frac{\partial^2 X_0}{\partial \tau^2} = -\frac{g}{\omega_0^2}, \quad \frac{\partial^2 Y_0}{\partial \tau^2} = 0 \tag{10.135}$$

$$\tau = \pm 1: \quad X_0 = 0, \quad Y_0 = 0, \quad \frac{\partial Y_0}{\partial \tau} = 0 \tag{10.136}$$

has solution

$$X_0 = \frac{g(1-\tau^2)}{2\omega_0^2}, \quad Y_0 = 0 \tag{10.137}$$

where condition (10.131) was taken into account.

Note that, in zero-order approximation, $\varepsilon = 0$, the physical assumption on energy loss, which is described by the boundary conditions (10.133), produced the equality $\partial Y_0/\partial \tau = 0$ at $\tau = \pm 1$in (10.136), which is satisfied automatically by the trivial solution for Y_0. Since the parameter ε itself characterizes the velocity drop at impact times, then the zero-order approximation $\varepsilon = 0$ cannot depict the effect of energy decay. This is why the dependence $\omega_0(\eta)$ still remains unknown and will be determined at the next step of asymptotic procedure.

Now taking into account (10.137) leads to the first-order boundary value problem

$$\begin{aligned}
\frac{\partial^2 X_1}{\partial \tau^2} &= -\frac{1}{\omega_0^2}\left(\frac{d\omega_0}{d\eta}\frac{\partial Y_0}{\partial \tau} + 2\omega_0 \frac{\partial^2 Y_0}{\partial \tau \partial \eta} + 2\omega_0\omega_1 \frac{\partial^2 X_0}{\partial \tau^2}\right) \\
&\equiv \frac{2g\omega_1}{\omega_0^3} \\
\frac{\partial^2 Y_1}{\partial \tau^2} &= -\frac{1}{\omega_0^2}\left(\frac{d\omega_0}{d\eta}\frac{\partial X_0}{\partial \tau} + 2\omega_0 \frac{\partial^2 X_0}{\partial \tau \partial \eta} + 2\omega_0\omega_1 \frac{\partial^2 Y_0}{\partial \tau^2}\right) \\
&\equiv -\frac{3g\tau}{\omega_0^4}\frac{d\omega_0}{d\eta}
\end{aligned} \tag{10.138}$$

$$\tau = \pm 1: \quad X_1 = 0, \quad Y_1 = 0 \tag{10.139}$$

whose solution is obtained by the direct integration as

$$X_1 = \frac{g\omega_1}{\omega_0^3}(\tau^2 - 1), \quad Y_1 = \frac{g}{2\omega_0^4}\frac{d\omega_0}{d\eta}(\tau - \tau^3) \tag{10.140}$$

Conditions of the velocity drop (10.133) combine now both zero- and first-order terms as

$$\tau = +1: \quad \omega_0 \left(\frac{\partial X_0}{\partial \tau} + \frac{\partial Y_0}{\partial \tau} - 2\frac{\partial Y_1}{\partial \tau} \right) - 2 \left(\frac{\partial X_0}{\partial \eta} + \omega_1 \frac{\partial Y_0}{\partial \tau} \right)$$

$$\equiv -\frac{g}{\omega_0^3} \left(\omega_0^2 - 2\frac{d\omega_0}{d\eta} \right) = 0 \tag{10.141}$$

$$\tau = -1: \quad \omega_0 \left(\frac{\partial X_0}{\partial \tau} - \frac{\partial Y_0}{\partial \tau} + 2\frac{\partial Y_1}{\partial \tau} \right) + 2 \left(\frac{\partial X_0}{\partial \eta} + \omega_1 \frac{\partial Y_0}{\partial \tau} \right)$$

$$\equiv \frac{g}{\omega_0^3} \left(\omega_0^2 - 2\frac{d\omega_0}{d\eta} \right) = 0 \tag{10.142}$$

It is seen that the quantity $\omega_1(\eta)$ disappears from these conditions, and both equalities are satisfied by just one separable differential equation

$$\frac{d\omega_0}{d\eta} = \frac{1}{2}\omega_0^2 \tag{10.143}$$

This gives zero-order approximation for the frequency function as

$$\omega_0 = \omega_0(0) \left[1 - \frac{1}{2}\omega_0(0)\eta \right]^{-1}, \quad \eta = \varepsilon t \tag{10.144}$$

Recall that the first-order term $\omega_1(\eta)$ has disappeared from the condition of velocity drop (10.141)–(10.142) and still remains arbitrary. As follows from (10.140), the term $\omega_1(\eta)$ determines the amplitude of approximation X_1. However, the parabolic shape described by the function $X_1(\tau)$ is already captured by zero-order approximation $X_0(\tau)$. Let us therefore take $X_1 \equiv 0$ by setting $\omega_1(\eta) \equiv 0$ as soon as no more steps of the asymptotic procedure will be conducted in present illustrating example. Note the discrete energy loss is described by function (10.144) in a continuous way by "corrupting" the temporal mode shape of the process $z(t)$ in between impact times. As a result, the Y-component of solution comes into play in order to correct such a side effect. This is clearly seen from solution (10.140) for Y_1, which would be zero if the quantity $\omega_0(\eta)$ was constant.

Now substituting both zero- and first-order approximations in (10.134) gives

$$z = \frac{g}{2\omega_0^2}(1 - \tau^2) \left(1 + \frac{1}{2}\varepsilon\tau e \right); \quad \tau = \tau(\varphi), \quad e = e(\varphi) \tag{10.145}$$

where $\omega_0 = \omega_0(\varepsilon t)$ is given by (10.144) and phase φ is determined by integration from the differential equation $\dot{\varphi}(t) = \omega_0(\varepsilon t)$.

Solution (10.145) links the initial height H to yet arbitrary $\omega_0(0)$ as

$$z(0) = \frac{g}{2[\omega_0(0)]^2} = H \quad \text{or} \quad \omega_0(0) = \sqrt{\frac{g}{2H}} \tag{10.146}$$

Finally, substituting ω_0 from (10.144) in solution (10.145) and taking into account (10.146) give

$$z(t) = H\left(1 - \frac{1}{2}\sqrt{\frac{g}{2H}}\varepsilon t\right)^2 \left(1 - \tau^2\right)\left(1 + \frac{1}{2}\varepsilon\tau e\right) \tag{10.147}$$

where $\tau = \tau(\varphi)$ and $e = e(\varphi)$ and the phase $\varphi = \varphi(t)$ is obtained from (10.144) by integration under the initial condition $\varphi(0) = 0$ in the form

$$\varphi = -\frac{2}{\varepsilon}\ln\left(1 - \frac{1}{2}\sqrt{\frac{g}{2H}}\varepsilon t\right) \tag{10.148}$$

As follows from solution (10.147) and (10.148), the bouncing process ends at

$$t_{\max} = \sqrt{\frac{2H}{g}}\frac{2}{\varepsilon} \tag{10.149}$$

Note that same result (10.149) was obtained in the reference [256] however, by using a different analytical tool based on the space unfolding coordinate transformation with averaging with respect the fast phase. Considering exact piecewise parabolic solution gives the duration of the bouncing process [73], which is in match with (10.149) when $0 < \varepsilon << 1$:

$$t_{\max} = \sqrt{\frac{2H}{g}}\frac{1+k}{1-k} = \sqrt{\frac{2H}{g}}\frac{2+\varepsilon}{\varepsilon} \sim \sqrt{\frac{2H}{g}}\frac{2}{\varepsilon}$$

However, temporal shapes of the above three solutions are somewhat different as it is seen from Fig. 10.22.

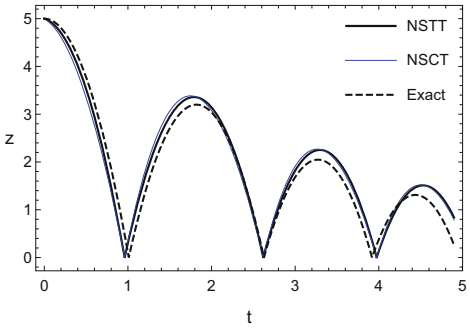

Fig. 10.22 Bouncing ball vertical coordinate versus time obtained by three different methods: nonsmooth temporal transformations (NSTT), nonsmooth coordinate transformation (NSCT), and exact solution